

**Influence of sepsis on cardiac metabolism and
function in dependence of intrinsic exercise capacity**

Dissertation

zur Erlangung des akademischen Grades

doctor medicinae (Dr. med.)

vorgelegt dem Rat der Medizinischen Fakultät

der Friedrich-Schiller-Universität Jena

von Jonas Marx

geboren am 11.03.1994 in Mühlhausen (Thüringen)

Gutachter

1. Prof. Dr. Torsten Doerst, Jena
2. Prof. Dr. Michael Bauer, Jena
3. PD Dr. Heiko Bugger, Graz/Österreich

Tag der öffentlichen Verteidigung: 03.09.2019

Content

Content.....	3
Abbreviations.....	5
Summary.....	7
Zusammenfassung	9
1 Introduction	11
1.1 SEPSIS AND SEPTIC CARDIOMYOPATHY	11
1.2 GENETIC PREDISPOSITION FOR INTRINSIC EXERCISE CAPACITY	12
1.3 INFLUENCE OF INTRINSIC EXERCISE CAPACITY ON SEPSIS SURVIVAL	13
1.4 CARDIAC SUBSTRATE METABOLISM IN HEALTH AND DISEASE	14
1.5 CARDIAC METABOLIC REGULATION BY INSULIN.....	15
1.6 CARNITINE PALMITOYLTRANSFERASES I AND II.....	16
1.7 INVESTIGATION OF CARDIAC METABOLISM USING RADIOACTIVE TRACER METHODS	18
2 Aims of the study	20
3 Materials	21
3.1 REAGENTS	21
3.2 DEVICES	22
3.3 PERFUSION APPARATUS	23
4 Methods.....	24
4.1 ANIMAL MODEL	24
4.1.1 <i>High and low capacity runners (HCR/LCR)</i>	24
4.1.2 <i>Induction of sepsis</i>	24
4.1.3 <i>Clinical severity score</i>	24
4.2 ISOLATED WORKING RAT HEART PERFUSION	25
4.2.1 <i>Isolated working rat heart preparation</i>	25
4.2.2 <i>Measurement of cardiac performance</i>	28
4.2.3 <i>Perfusion protocol</i>	28

4.3 RADIOISOTOPIC TECHNIQUES	29
4.3.1 Determination of glucose oxidation.....	29
4.3.2 Determination of fatty acid oxidation.....	30
4.4 TISSUE CHEMISTRY AND PHOTOMETRIC METHODS	31
4.4.1 Carnitine palmitoyltransferase I/II activity.....	31
4.4.2 Bradford protein assay.....	32
4.4.3 Cardiac dry weight	32
4.5 STATISTICAL ANALYSIS	33
5 Results	34
5.1 MORPHOLOGY.....	34
5.2 CARDIAC POWER	35
5.3 CARDIAC PERFORMANCE PARAMETERS	36
5.4 BASELINE CARDIAC GLUCOSE OXIDATION	37
5.5 INSULIN STIMULATED CARDIAC GLUCOSE OXIDATION	38
5.6 BASELINE CARDIAC FATTY ACID OXIDATION	39
5.7 INSULIN STIMULATED CARDIAC FATTY ACID OXIDATION	40
5.8 RATIO OF GLUCOSE OXIDATION TO FATTY ACID OXIDATION	41
5.9 CARDIAC EFFICIENCY	42
5.10 CARNITINE PALMITOYLTRANSFERASE I AND II ACTIVITY	43
6 Discussion.....	44
7 Conclusion.....	50
8 References	51
9 Appendix	58
9.1 LIST OF FIGURES.....	58
9.2 EHRENWÖRTLICHE ERKLÄRUNG	59
9.3 ACKNOWLEDGEMENT	60

Abbreviations

ATP	adenosine triphosphate
ANOVA	analysis of variance
BSA	bovine serum albumin
CLP	cecal ligation and puncture
CoA	coenzyme A
CPT I	carnitine palmitoyltransferase I
CPT II	carnitine palmitoyltransferase II
CSS	clinical severity score
DTNB	5,5'-dithiobis-2-nitrobenzoic
EDTA	ethylenediaminetetraacetic acid
FADH ₂	flavin adenine dinucleotide
FAO	fatty acid oxidation
GO	glucose oxidation
GO/FAO	ratio of glucose oxidation to fatty acid oxidation
GLUT4	glucose transporter 4
HCR	high capacity runners
HEPES	4-(2-hydroxyethyl)-1-piperazineethanesulfonic acid
IR	insulin resistance
IRS-1	insulin receptor substrate 1
KH	Krebs-Henseleit
LCR	low capacity runners
LPS	lipopolysaccharide

LVEF	left ventricular ejection fraction
NADH	nicotinamide adenine dinucleotide
PCI	peritoneal contamination and infection
PDH	pyruvate dehydrogenase
PI3K	phosphatidylinositol 3-kinase
SCM	septic cardiomyopathy
TCA	tricarboxylic acid cycle
TNF- α	tumor necrosis factor alpha

Summary

Background: Sepsis, defined as life-threatening organ dysfunction caused by a dysregulated host response to infection, represents a global health issue due to high prevalence and mortality. Manifestation of septic cardiomyopathy (SCM), one of many complications in sepsis, is associated to a worse outcome. The molecular features of SCM and septic effects on cardiac metabolism are not sufficiently characterized. Genetic predisposition for exercise capacity may be one factor influencing the course of sepsis. Sepsis-survival experiments with high capacity runners (HCR) and low capacity runners (LCR), a rat model for intrinsic exercise capacity, linked high exercise capacity to an advantage in survival 24 h after sepsis induction. The reasons for this advantage are unknown. We intend to identify potential sepsis-related alterations of cardiac metabolism and function that may be responsible for the mentioned findings and aim to uncover new metabolic mechanisms involved in the development of sepsis-associated cardiac dysfunction.

Methods: Sepsis was induced by intraperitoneal injection of a pooled human stool sample in male HCR and LCR rats at the age of 15 weeks. Isolated working heart perfusions were performed without sepsis induction as well as 24-36 h, 4-5 d and 4-5 w after sepsis induction with modified Krebs-Henseleit buffer containing glucose (5 mM) and sodium oleate (0.4 mM) bound to 1% bovine serum albumin (BSA). [U- ^{14}C]-glucose and [9,10- ^3H]-oleate were added to the perfusion medium to assess cardiac glucose and fatty acid oxidation. After 30 min of baseline perfusion, insulin was administered to evaluate cardiac insulin sensitivity. Cardiac function and performance were monitored continuously throughout the experiment. Morphological parameters of the rats including body and heart weight were recorded. Enzymatic activities of carnitine palmitoyltransferase I and II were determined using a spectrophotometric method.

Results: LCR rats weighed significantly more than HCR rats. A similar tendency was observed for heart weights. Cardiac performance assessed *ex vivo* during isolated working heart perfusions was neither compromised in acute sepsis nor in sepsis-survivors and did not depend on intrinsic exercise capacity. LCR hearts tended to oxidize more glucose and less

oleate than HCR hearts. Acute sepsis and survival of sepsis were not associated to relevant alterations of basal cardiac substrate oxidation. Insulin sensitivity was preserved in all groups at all investigated time points, indicated by a robust increase of glucose oxidation and decrease of fatty acid oxidation after insulin stimulation. Carnitine palmitoyltransferase I and II activities were not changed during sepsis and were not influenced by intrinsic exercise capacity.

Conclusion: Sepsis did not induce substantial disturbances of cardiac metabolism or function. Genetic predisposition for intrinsic exercise capacity did not affect cardiac substrate oxidation during acute sepsis or in sepsis-survivors. We conclude that the detrimental effects of sepsis cannot be attributed to metabolic or mechanical dysfunction of the heart in our model. The mechanisms mediating the advantage in 24 h survival associated to high intrinsic exercise capacity remain elusive.

Zusammenfassung

Hintergrund: Die Sepsis, definiert als eine lebensbedrohliche Organdysfunktion verursacht durch eine überschießende Immunantwort des Organismus auf eine Infektion, stellt ein globales Gesundheitsproblem mit hoher Prävalenz und Mortalität dar. Das Auftreten einer septischen Kardiomyopathie (SCM), einer der vielen Komplikationen im Rahmen der Sepsis, ist mit einem ungünstigeren Krankheitsverlauf assoziiert. Die molekularen Eigenschaften der SCM und Effekte der Sepsis auf den Herzstoffwechsel generell sind nicht hinreichend charakterisiert. Ein Faktor, der den Verlauf einer Sepsis beeinflussen könnte, ist die genetische Prädisposition für intrinsische Leistungskapazität. In Versuchen mit septischen Ratten mit hoher (HCR) und niedriger (LCR) intrinsischer Leistungskapazität zeigte sich, dass Tiere mit hoher Leistungskapazität Vorteile im Überleben 24 h nach Sepsisinduktion aufwiesen. Die Ursachen dieses Überlebensvorteils blieben unklar. Die vorliegende Arbeit zielt darauf ab, potentielle Veränderungen von Herzstoffwechsel und -funktion im Rahmen einer Sepsis zu beschreiben, die möglicherweise mitverantwortlich für die festgestellten Unterschiede im Überleben sind, und neue metabolische Mechanismen zu entdecken, welche zur Entwicklung einer Sepsis-assoziierten kardialen Dysfunktion beitragen.

Methoden: In männlichen HCR und LCR Ratten im Alter von 15 Wochen wurde eine Sepsis durch intraperitoneale Injektion einer gepoolten humanen Stuhlsuspension induziert. Nach 24-36 h, 4-5 d und 4-5 w wurden die Ratten euthanasiert, um isoliert arbeitende Herzperfusionen mit modifiziertem Krebs-Henseleit-Buffer, angereichert mit Glukose (5 mM) und Oleat (0.4 mM) gebunden an 1% BSA, durchzuführen. [U- ^{14}C] -Glukose und [9,10- ^3H] -Oleat wurden dem Perfusionsmedium zugegeben, um den kardialen Glukose- und Fettsäurestoffwechsel quantitativ einzuschätzen. Nach einer Perfusionszeit von 30 min zur Messung der basalen Substratoxidation wurde Insulin zur Bewertung der kardialen Insulinsensitivität in das Perfusionssystem gegeben. Herzfunktion und -leistung wurden kontinuierlich während der Perfusion aufgezeichnet. Morphologische Parameter der Ratten einschließlich Körper- und Herzgewicht wurden protokolliert. Die enzymatische Aktivität der Carnitin-Palmitoyltransferasen I und II, isoliert aus Herzgewebe, wurden spektrophotometrisch bestimmt.

Ergebnisse: Das Körpergewicht von LCR Ratten war signifikant größer im Vergleich zu HCR Ratten. Eine ähnliche Tendenz zeigte sich für das Herzgewicht. Die *ex vivo* während der Herzperfusion gemessene Herzleistung war weder in der akuten Sepsis noch in Sepsis-Überlebenden beeinträchtigt und hing nicht von der intrinsischen Leistungskapazität ab. LCR Herzen neigten verglichen mit HCR Herzen zu einer höheren Glukoseoxidation und einer niedrigeren Fettsäureoxidation. Akute Sepsis oder das Überleben einer Sepsis hatten keinen wesentlichen Einfluss auf die basale Substratoxidation des Herzens. Die Gabe von Insulin provozierte in allen untersuchten Gruppen einen adäquaten Anstieg von Glukoseoxidation und einen Abfall der Fettsäureoxidation. Dies weist auf eine erhaltene kardiale Insulinsensitivität während und nach einer Sepsis unabhängig von der angeborenen Leistungskapazität hin. Die enzymatischen Aktivitäten der Carnitin-Palmitoyltransferasen I und II zeigten sich 24 h nach Sepsisinduktion nicht verändert und unterschieden sich nicht zwischen HCR und LCR Herzen.

Schlussfolgerung: Die Sepsis zeigte in dieser Studie keine wesentlichen Auswirkungen auf Herzstoffwechsel oder -leistung. Die genetische Prädisposition für intrinsische Leistungskapazität hatte weder während der akuten Sepsis noch in Sepsis-Überlebenden signifikanten Einfluss auf die kardiale Substratoxidation. Damit können die in unserem Sepsis-Model präsente hohe Mortalität und die ausgeprägte gesundheitliche Beeinträchtigung nicht auf Dysfunktionen des kardialen Stoffwechsels oder der kontraktile Herzfunktion zurückgeführt werden. Die Mechanismen, die den signifikanten Überlebensvorteil von HCR Ratten gegenüber LCR Ratten 24 h nach Sepsisinduktion vermitteln, bleiben weiterhin unklar.

1 Introduction

1.1 Sepsis and septic cardiomyopathy

While the origins of the term sepsis can be traced back to ancient times, it was the German physician Hugo Schottmüller who introduced the first modern definition of sepsis, recognizing bacterial infection as an essential part of the disease (Schottmüller 1914): "Sepsis is present if a focus has developed from which pathogenic bacteria, constantly or periodically, invade the blood stream in such a way that this causes subjective and objective symptoms." Since then, our knowledge about pathomechanisms and nature of sepsis steadily increased and new definitions evolved over time. The most recent was developed by an international task force in 2016 (sepsis-3), defining sepsis as life-threatening organ dysfunction caused by a dysregulated host response to infection (Singer et al. 2016). Thereby, not only the infection but also the overshooting inflammatory host response and consecutive organ dysfunction characteristic for sepsis were accounted for.

Despite immense scientific efforts to combat the detrimental consequences of septic infections, sepsis remains a major health issue on national and global level. In 2013, 279530 cases of sepsis were registered in German hospitals (Fleischmann et al. 2016). The in-hospital mortality was determined as 24.3%, corresponding to 67849 sepsis-associated deaths. In comparison to 2007, the incidence of sepsis rose by an average of 5.7% per year. Alarmingly, mortality only dropped by a total of 2.7% over the same period. A comparable trend was reported by the National Center for Health Statistics for the USA, underlining the international relevance of sepsis (Hall et al. 2011). The annual incidence of sepsis rose by 70% from 22.1 per 10000 in 2000 to 37.7 per 10000 in 2008.

Sepsis can interfere with the function of a variety of organ systems, including the heart. Manifestation of septic cardiomyopathy (SCM), broadly defined as an acute syndrome of cardiac dysfunction in patients with sepsis (Beesley et al. 2018), is considered a serious complication. The prevalence of SCM varies around 50% depending on the method applied to identify cardiac dysfunction. Early studies defined SCM as a depression of left ventricular ejection fraction (LVEF) concomitant with ventricular dilation (Parker et al. 1984). However, LVEF is influenced by several factors, such as cardiac filling pressure and afterload, and may

not reflect intrinsic cardiac function. Additionally, LVEF was found to be a poor predictor of mortality in septic patients (Sevilla Berrios et al. 2014). Recently, longitudinal strain, a measure of the deformation of the myocardium detected by echocardiography, was suggested to be a more sensitive parameter for cardiac dysfunction compared to LVEF (Stanton et al. 2009). Indeed, pathologic left ventricular longitudinal strain was found in septic patients and correlated significantly with mortality (Palmieri et al. 2015). Regardless of the diagnostic tool, most studies associate SCM to a worse outcome of sepsis.

The causative mechanisms involved in the development of SCM are under constant debate. A variety of chemical mediators has been proposed to induce SCM. Tumor necrosis factor alpha and interleukin 1 beta, cytokines significantly up-regulated in acute sepsis, were shown to depress myocardial cell contractility with a synergistic effect *in vitro* (Kumar et al. 1996). Oxidative damage due to increased production of reactive oxygen species was linked to compromised cardiac function in sepsis (Tsolaki et al. 2017, Khadour et al. 2002). Furthermore, excess production of nitric oxide caused by elevated levels of inducible nitric oxide synthase was associated to cardiac impairment in septic animal models (Khadour et al. 2002, Preiser et al. 2001). Unfortunately, the suggested mechanisms did not translate into improvements of clinical therapy yet, hinting on additional factors contributing to the manifestation of SCM. So far, alterations of cardiac substrate metabolism in SCM have been rather neglected. Since cardiac function and oxidative substrate metabolism are inextricably linked, potential disturbance of metabolic pathways in the septic heart may lead to mechanical dysfunction. Thus, a better understanding of cardiac metabolism in sepsis is mandatory and may grant access to new therapeutic strategies.

1.2 Genetic predisposition for intrinsic exercise capacity

Development and outcome of diseases are determined by a plethora of extrinsic and intrinsic factors. Among the intrinsic, the genetic predisposition for exercise capacity appears to play an interesting role. In order to study intrinsic exercise capacity under controlled and reproducible conditions, Britton and Koch generated an innovative rat model (Koch et al. 1998, Koch und Britton 2001). Outbred N:NIH rats were tested for their running performance on a treadmill. Based on the results, the highest-performing rats and lowest-performing rats were selected and bred separately. Repetition of this strategy for more than 20 generations led to two populations (high capacity runners, HCR, and low capacity runners, LCR)

substantially differing in their physical exercise capacity (Figure 1), illustratively measured as distance run to exhaustion, maximal speed and time run to exhaustion (Schwarzer et al. 2010).

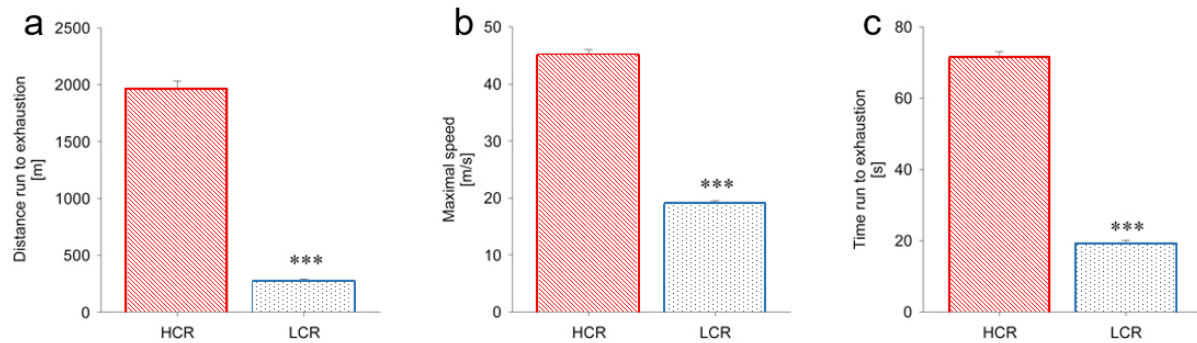


Figure 1: Exercise performance assessed in HCR and LCR rats after 22 generations of divergent selection. HCR – high capacity runners, LCR – low capacity runners (Schwarzer et al. 2010).

Besides differences in physical endurance, HCR and LCR rats showed divergent characteristics in several other domains. Interestingly, low intrinsic exercise capacity was associated to a decreased lifespan compared to high exercise capacity (Koch et al. 2011). Blood pressure, fasting glucose, serum insulin, serum triglycerides and free fatty acids were significantly increased in LCR compared to HCR, indicating an unfavorable cardiovascular and metabolic phenotype (Wisloff et al. 2005). LCR rats exhibit systemic insulin resistance (IR), most pronounced after challenge with high-fat diet (Bikman et al. 2009, Noland et al. 2007). In a study investigating nociception, HCR displayed higher pain thresholds, indicating a lower susceptibility to painful stimuli compared to LCR (Geisser et al. 2008).

1.3 Influence of intrinsic exercise capacity on sepsis survival

As demonstrated, HCR/LCR represents a complex genetic model for intrinsic exercise capacity which results in divergent phenotypes. We questioned how the genetic predisposition for intrinsic fitness would influence the development and outcome of a complex disease, such as sepsis. In a pilot study, sepsis was induced in male HCR and LCR rats by intraperitoneal injection of a pooled human stool sample. The animals were closely monitored for signs of illness and death to perform a survival analysis. Indeed, 24 h after sepsis induction HCR rats

presented with a significant advantage in survival compared to LCR (Figure 2). However, this advantage was blunted 72 h after sepsis induction and total mortality appeared indifferent.

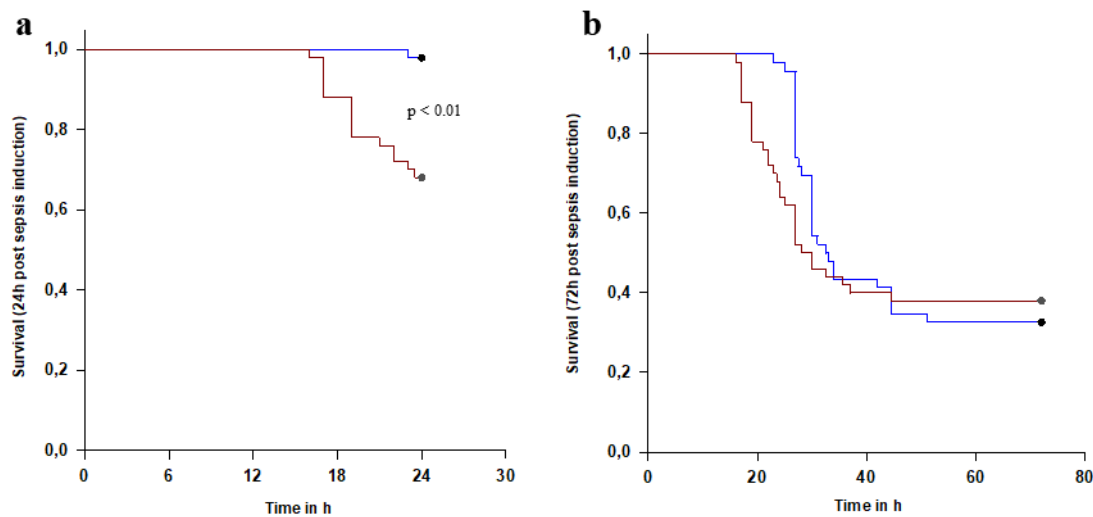


Figure 2: Influence of intrinsic exercise capacity on sepsis survival. High capacity runners (HCR, —) and low capacity runners (LCR, —). Log-rank test. Unpublished data.

The reasons for the significant advantage in survival 24 h after sepsis induction for HCR rats were not apparent. We decided to follow-up on these interesting findings and hypothesized that impairment of cardiac function or perturbation of cardiac substrate metabolism during the acute phase of sepsis may be of importance for the observed difference in survival.

1.4 Cardiac substrate metabolism in health and disease

The heart relies on a continuous and efficient supply of adenosine triphosphate (ATP) to sustain mechanical function. Physiologically, ATP formation in adult cardiomyocytes is predominantly fueled by oxidation of fatty acids (Neely und Morgan 1974, Saddik und Lopaschuk 1991, Doenst et al. 2013). However, the heart is characterized by substantial metabolic flexibility and was therefore aptly considered an ‘omnivore’ (Taegtmeyer und Lubrano 2014). Dependent on metabolic regulation and availability of resources, cardiac substrate preference may shift from fatty acid towards glucose consumption, and other substrates, such as lactate, pyruvate or ketone bodies, may contribute to cardiac ATP

formation to a larger extent. This versatility guarantees sufficient cardiac energy supply under varying conditions and ensures maintenance of contractile function.

Interestingly, different types of cardiac disease, e.g., ischemic heart failure, are accompanied by derangements of cardiac substrate metabolism and restriction of metabolic flexibility (Doenst et al. 2013, Karwi et al. 2018). In the failing heart, compromised mitochondrial function and impaired oxidative phosphorylation lead to a lack of ATP production (Neubauer 2007). While oxidation of fatty acids is the main source of ATP generation in the healthy heart, the majority of studies report a decrease of fatty acid oxidation already in early stages of heart failure (Doenst et al. 2010, Akki et al. 2008). Similarly, glucose oxidation was observed to be decreased in several models of heart failure (Zhabyeyev et al. 2013, Mori et al. 2012). However, the findings were inconsistent as some studies reported unchanged or increased rates of glucose oxidation (Doenst et al. 2010, Karwi et al. 2018). The general decline of oxidative ATP production was, in many cases, met by a shift towards anaerobic metabolism, i.e., flux through anaerobic glycolysis was elevated in hypertrophic hearts (Allard et al. 1994, Riehle et al. 2011).

Thus, pathological alterations of cardiac function and structure are associated to profound metabolic remodeling. Unfortunately, studies addressing metabolic changes and cardiac substrate preference in septic hearts are scarce and conflicting. In C57BL/6 mice subjected to injection of LPS to induce endotoxemia, palmitate oxidation was significantly depressed (Drosatos et al. 2011). In a similar model, both fatty acid oxidation and glucose oxidation were markedly suppressed after LPS administration (Drosatos et al. 2013). In contrast, fractional contribution of fatty acid oxidation to ATP production was increased in mice 24h after sepsis induction by cecal ligation and puncture (Standage et al. 2017). Additional investigations focusing on cardiac substrate metabolism and metabolic regulation are required to gain a better understanding of the pathophysiology of septic cardiomyopathy.

1.5 Cardiac metabolic regulation by insulin

Cardiac substrate metabolism is controlled by a plethora of mechanisms. Amongst hormonal regulators, insulin represents one of the most influential factors for cardiac substrate selection (Bertrand et al. 2008). After binding of insulin to the extracellular part of the insulin receptor, a cascade of reactions is activated. In brief, binding of insulin prompts the autophosphorylation of the insulin receptor and phosphorylation of further substrates, such as

insulin receptor substrate and Shc. Consequential, phosphatidylinositol 3-kinase (PI3K) is activated. PI3K phosphorylates phosphatidylinositol (4,5)-bisphosphate to phosphatidylinositol (3,4,5)-trisphosphate which recruits and activates phosphoinositide-dependent kinase 1 and protein kinase B/Akt. The colocalization and action of the latter ultimately provokes a series of metabolic effects. First, glucose transporter 4 (GLUT4) is translocated from intracellular vesicles to the sarcolemmal membrane, enabling increased glucose uptake into the cardiomyocytes. Second, insulin signaling stimulates the synthesis of fructose 2,6-bisphosphate, a key activator of phosphofructokinase-1, leading to higher flux through glycolysis (Bertrand et al. 2008). As glucose utilization is favored after insulin stimulation, fatty acid oxidation contributes less to ATP production.

Some evidence suggests interference of the inflammatory milieu present in sepsis with systemic insulin signaling. Various studies reported systemic insulin resistance in the context of sepsis and endotoxemia (Illuri et al. 2016, Marik und Raghavan 2004, Agwunobi et al. 2000). Importantly, the finding of systemic insulin resistance does not necessarily translate to insulin resistance of cardiomyocytes. Indeed, most experiments primarily demonstrated impaired insulin signaling in peripheral tissues, such as skeletal muscle, adipose tissue or liver (Bierbrauer und Weber-Carstens 2011, McCowen et al. 2001). In open-chest pentobarbital sodium-anesthetized dogs, cardiac insulin sensitivity was found to be reduced in hyperinsulinemic-euglycemic clamp experiments after endotoxin administration (Raymond et al. 1988). Likewise, bacterial endotoxin injection in rats induced a reduction of cardiac glycolysis and glycogen synthesis after insulin stimulation compared to control, indicating endotoxin mediated insulin resistance (Tessier et al. 2003). Admittedly, both studies used the rather artificial experimental setup of direct LPS infusion to generate endotoxemia. Therefore, it remains of great interest if impaired cardiac insulin signaling is also present in more physiological models of sepsis.

1.6 Carnitine palmitoyltransferases I and II

While glucose utilization is in part directed by insulin signaling, different mechanisms apply on the regulation of fatty acid oxidation. An essential and rate-limiting step of oxidative fatty acid metabolism is the transfer of activated fatty acids into the mitochondrial matrix, the cellular compartment containing the enzymatic machinery required for β -oxidation. This transport is facilitated by an enzyme system involving carnitine palmitoyltransferase I and II

(CPT I and CPT II) (Park und Cook 1998). After incorporation of fatty acids into the cytosol, they are activated to acyl-CoA thioesters by acyl-CoA synthetase. CPT I, located in the outer mitochondrial membrane, transfers the acyl groups from CoA to carnitine to produce acylcarnitine (Figure 3). Acylcarnitine is transported into the mitochondrial matrix in exchange for free carnitine by carnitine-acylcarnitine translocase. Finally, CPT II, located in the inner mitochondrial membrane, reconverts acylcarnitine to acyl-CoA to complete the transfer. As for enzymatic regulation, malonyl-CoA, a substrate for fatty acid synthase and indicator of high levels of acetyl-CoA, represents a potent inhibitor of CPT I specifically (Paulson et al. 1984). Thus, fatty acid oxidation is limited in situations of energy overload and metabolic efficiency is improved.

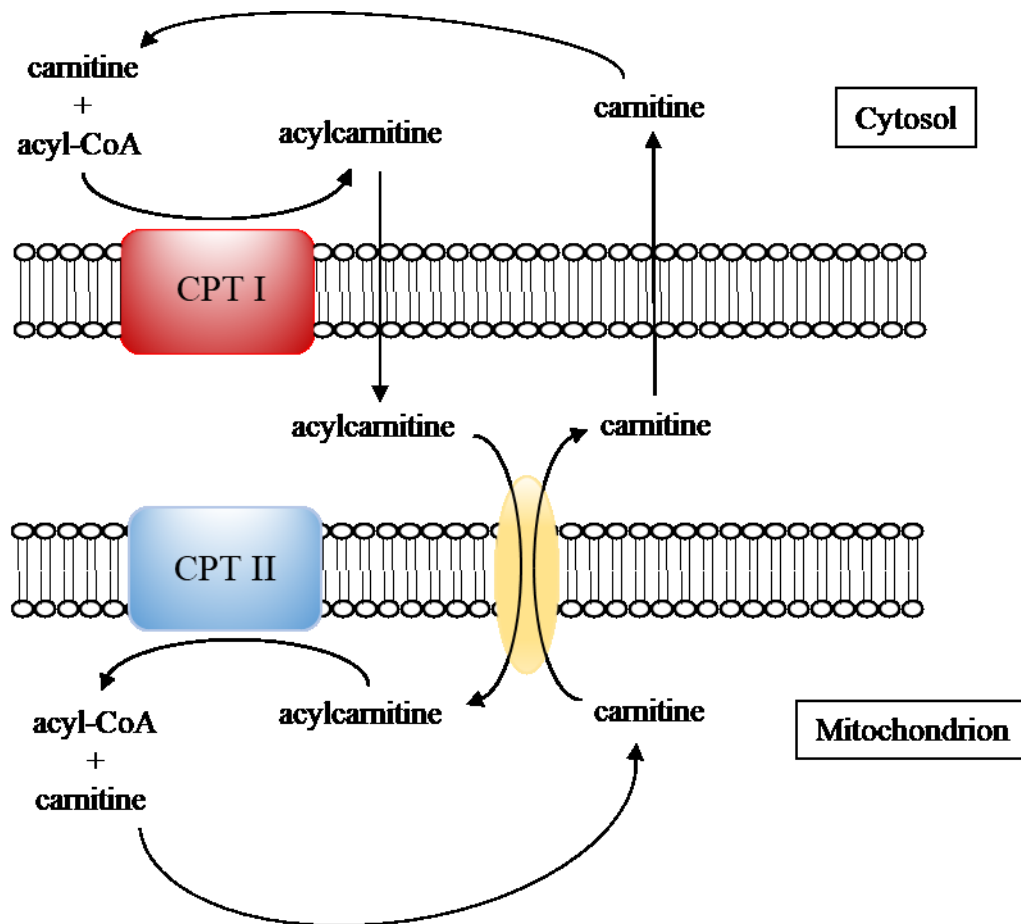


Figure 3: Carnitine palmitoyltransferase system. CPT I – carnitine palmitoyltransferase I, CPT II - carnitine palmitoyltransferase II, yellow ellipse represents carnitine-acylcarnitine translocase.

Interestingly, CPT I activity appears to be affected by inflammatory mediators. Suckling rats received LPS intraperitoneally to induce neonatal endotoxemia. As a consequence, cardiac CPT I activity was significantly decreased, possibly due to increased nitration of the CPT I enzyme (Fukumoto et al. 2002, Eaton et al. 2003). Further experiments are mandatory to determine if the observed effects are also present in adult organisms and to confirm the results in different models of sepsis.

1.7 Investigation of cardiac metabolism using radioactive tracer methods

The assessment of cardiac substrate oxidation requires advanced techniques. One approach to determine metabolic flux rates in the heart is the use of instable, radioactive tracers (Taegtmeyer et al. 2016). In principle, stable atoms of energy-providing substrates are replaced by radioactive isotopes, such as ^{14}C , ^3H or ^{32}P . When labeled substrates are metabolized, new labeled metabolites and metabolic byproducts are formed which can be analyzed and quantified to estimate flux through the respective pathway. While radioactive tracers can be used in a broad range of test systems, only the application in isolated beating heart experiments allows the cardiac-specific determination of substrate oxidation independent of the remaining organism. For that reason, a variety of tracer protocols for isolated perfused heart experiments have been established and successfully applied over the past decades (Goodwin et al. 1998, Doenst et al. 1999).

In this study, we used $[\text{U-}^{14}\text{C}]$ -glucose and $[9,10\text{-}^3\text{H}]$ -oleate to assess oxidative cardiac substrate metabolism (Goodwin et al. 1998, Nguyen et al. 2015). After uptake into the cell, $[\text{U-}^{14}\text{C}]$ -glucose is metabolized to $[\text{U-}^{14}\text{C}]$ -pyruvate by glycolysis which is transported into the mitochondrion (Figure 4). Here, $[\text{U-}^{14}\text{C}]$ -pyruvate is decarboxylated to $[\text{U-}^{14}\text{C}]$ -acetyl-CoA by pyruvate dehydrogenase, resulting in the release of ^{14}C -labeled CO_2 . During the oxidation of $[\text{U-}^{14}\text{C}]$ -acetyl-CoA within the tricarboxylic acid cycle, another two $^{14}\text{CO}_2$ molecules are liberated. Isolation and quantification of the released $^{14}\text{CO}_2$ allows the calculation of absolute glucose oxidation.

In an initial cytosolic reaction, $[9,10\text{-}^3\text{H}]$ -oleate is activated to $[9,10\text{-}^3\text{H}]$ -oleyl-CoA. Hereafter, the activated compound is transported over the mitochondrial membrane by action of carnitine palmitoyltransferases I and II, the rate-limiting step of fatty acid oxidation. In the mitochondrion, $[9,10\text{-}^3\text{H}]$ -oleyl-CoA is broken down to acetyl-CoA units by β -oxidation. This

process leads to the release of ^3H -labeled water. Isolation and quantification of $^3\text{H}_2\text{O}$ enables the estimation of absolute oleate oxidation.

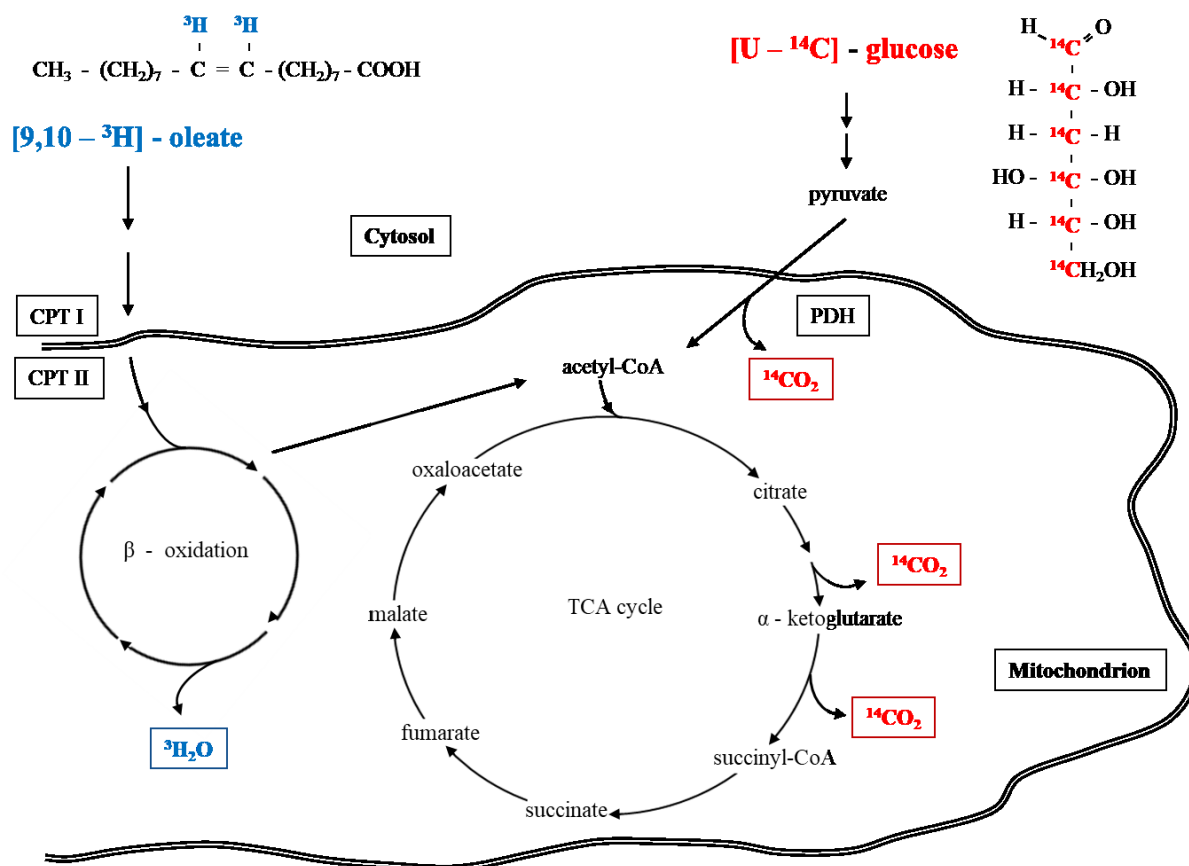


Figure 4: Biochemistry of the radioactive tracers [U- ^{14}C]-glucose and [9,10- ^3H]-oleate. CoA – coenzyme A, PDH – pyruvate dehydrogenase, CPT I/II – carnitine palmitoyltransferase I and II, TCA – tricarboxylic acid.

2 Aims of the study

The molecular features of SCM or septic effects on cardiac metabolism in general have not been completely characterized and understood. Initial survival experiments with HCR and LCR rats demonstrated that high intrinsic exercise capacity is associated to a significant advantage in survival in the first phase of sepsis, i.e., 24 h hours after sepsis induction. The reasons responsible for the improved survival remained elusive.

Based on the current lack of knowledge, we addressed the following questions in the present study:

- Does the genetic predisposition for intrinsic exercise capacity influence cardiac glucose and fatty acid metabolism during acute sepsis?
- Does sepsis induce changes in cardiac insulin sensitivity in dependence of exercise capacity?
- Are cardiac CPT I and II activities affected by the inflammatory milieu in septic animals?
- Are cardiac performance and mechanical function compromised 24h after sepsis induction?
- Are permanent changes of cardiac metabolism and function present in sepsis survivors?

A better understanding of potential cardiac metabolic and functional alterations induced by sepsis might open new perspectives on future therapy strategies and treatment regimens.

3 Materials

3.1 Reagents

Reagent	Source of supply
5,5'-dithiobis-2-nitrobenzoic acid	Sigma
1-X8 resin chloride form	Bio-Rad Laboratories
Benzethonium hydroxide	Sigma
Bovine serum albumin	Sigma
Bovine serum albumin protein standard	Sigma
Calcium chloride	Merck
L-carnitine	Sigma
Dihydrogen potassium phosphate	Merck
EDTA	Roth
Glucose	Sigma
[U- ¹⁴ C]-glucose	Perkin-Elmer
Heparin-Natrium-25000	Ratiopharm
HEPES	Sigma
Insulin (Insuman® Rapid)	Sanofi-Aventis
Magnesium chloride	Sigma
Magnesium sulfate	Merck
Malonyl-Coenzyme A	Sigma
Methanol	Roth
[9,10- ³ H]-oleic acid	Perkin-Elmer

Palmitoyl-Coenzyme A	Sigma
Perchloric acid	Merck
Potassium chloride	Roth
Protein Assay Dye Reagent	Bio-Rad Laboratories
Sodium bicarbonate	Roth
Sodium chloride	Roth
Sodium oleate	Sigma
Sodium thiopental	Inresa
Tris-Base	Roth
Tris-Cl	Roth
Triton™ X-100	Sigma
Ultima Gold™ scintillation cocktail	PerkinElmer

3.2 Devices

Device	Source of supply
Multipurpose scintillation counter LS 6500	Beckman
Centrifuge 5804 R	Eppendorf
Sonicator UW 2070	BANDELIN electronic
Synergy 2 Multi-Mode Microplate Reader	BioTek Instruments
Teflon homogenizer RE 16	IKA-Labortechnik

3.3 Perfusion apparatus

Device	Source of supply
Pressure transducer and recording system	Millar Instruments
Perfusion glassware	P.A. Brooks, Prototype Scientific Glass Blower
Tygon™ tubing 3.2 mm x 0.8 mm, 15 m	Saint Gobain
Tygon™ tubing 6.4 mm x 1.6 mm, 15 m	Saint Gobain
Glass Fiber filter APFD04700	Millipore
Mixed cellulose esters membrane SMWP04700	Millipore

4 Methods

4.1 Animal model

4.1.1 High and low capacity runners (HCR/LCR)

Rats selectively bred for high (HCR) and low capacity running (LCR) have been obtained from Steve Britton and Lauren Koch, Department of Anesthesiology, University of Michigan, Ann Arbor, Michigan, USA. The animals have been bred and housed at the Department of Laboratory Animal Science, University Jena, Germany under artificial day-night conditions (12 h light, 12 h dark) at room temperature. Water and food were available ad libitum. All experiments were approved by the regional animal welfare committee and were performed according to the German legislation on protection of animals.

4.1.2 Induction of sepsis

Sepsis was induced in male HCR and LCR rats at the age of 15 ± 1 weeks using a standardized peritoneal contamination and infection model (Gonnert et al. 2011, Chung et al. 2017). Under mild anesthesia (isoflurane 2%), a stool suspension (0.8 μ l/g body weight) was injected intraperitoneally into the right lower quadrant of the abdomen with a 21-gauge cannula. The stool suspension derived from pooled human stool samples was provided by the Department of Experimental Anesthesiology, University Hospital Jena, Germany.

4.1.3 Clinical severity score

After induction of sepsis, the animals were monitored using the clinical severity score (CSS), an assessment system developed previously (Gonnert et al. 2011). The CSS considers spontaneous activity, reaction to exogenous stimuli and posture to evaluate the clinical status. Table 1 lists the assessed items in detail.

Table 1: Clinical severity score (CSS) for the assessment of the clinical status (Gonnert et al. 2011).

Grade	Criteria		
	Spontaneous activity	Reaction to exogenous stimuli	Posture
1	Active, strong	Curious, quick movements	Normal
2	Less active with occasional interruptions in activity	Reduced alertness, but adequate response	Slightly hunched
3	Slow, sleepy moves with difficulty	Limited and delayed	Hunched
4	Lethargic, motionless, no movement	None	Severely hunched

4.2 Isolated working rat heart perfusion

4.2.1 Isolated working rat heart preparation

Hearts of HCR and LCR rats were perfused before sepsis induction (control) as well as 24-36 h, 4-5 d and 4-5 w after sepsis induction. The set of perfusions performed after 24-36 h was meant to assess acute changes of cardiac metabolism and *ex vivo* cardiac performance during sepsis. Experiments after 4-5 d and 4-5 w addressed potential intermediate- and long-term alterations of cardiac substrate utilization and function in sepsis survivors. Isolated working rat hearts were prepared as described previously with some modifications (Doenst et al. 1998, Doenst et al. 1999). Rats were anesthetized with sodium thiopental (5 mg/100g body weight, intraperitoneal injection). When deep anesthesia was ensured, a transverse abdominal cut was done to expose the inferior vena cava. 200 IU heparin were injected into the inferior vena cava. Median sternotomy was followed by rapid excision of the heart-lung-package. Immediately after excision, the heart was placed in ice-cold Krebs-Henseleit (KH) buffer (128 mM NaCl, 5 mM KCL, 1 mM KH₂PO₄, 1.3 mM MgSO₄, 15 mM NaHCO₃,

2.5 mM CaCl_2) to prevent ischemic damage. The aorta was freed from excess tissue and cannulated. A brief period of retrograde perfusion (Langendorff mode) allowed to wash out any blood remaining in the heart and to cannulate the left atrium. After successful cannulation, the hearts were placed in the heart chamber connected to a compliance unit and perfused as working hearts with recirculating KH medium containing glucose (5 mM) and sodium oleate (0.4 mM) bound to 1% BSA. Figure 5 schematically demonstrates the experimental setup. The perfusion medium was equilibrated with 95% O_2 – 5% CO_2 . Temperature was maintained at 37°C. A preload of 15 cmH₂O and an afterload of 100 cmH₂O were guaranteed for all experiments. Hearts were beating spontaneously without requirement of a pacemaker. Body weights and organ weights were recorded.

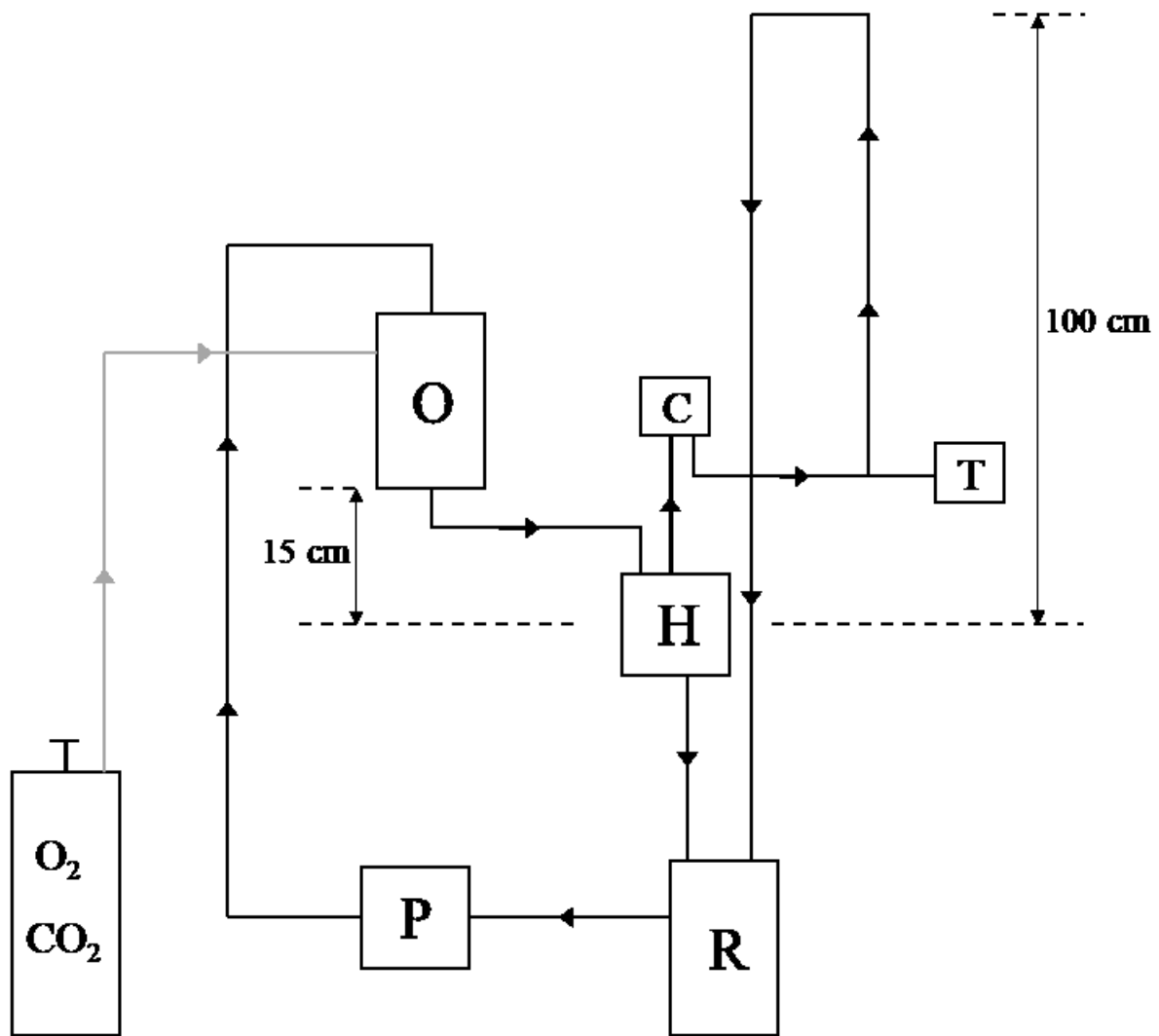


Figure 5: Experimental setup of the isolated working rat heart. H – heart chamber with isolated working heart, C – compliance unit, T – pressure transducer and recording system, R – reservoir for perfusion medium, P – pump to recirculate medium, O – oxygenator. Arrows hint on the direction of flow. Preload (15 cm H_2O) and afterload (100 cm H_2O) are indicated.

4.2.2 Measurement of cardiac performance

Cardiac mechanical function, including heart rate and left ventricular contractility (+dP/dt), was monitored continuously by a pressure transducer connected to a recording system (Millar Instruments, Houston). Aortic and coronary flow were measured every 5 min by timing the rise of the respective fluid meniscus in calibrated sections of the perfusion system. Cardiac power was calculated according to the basic physical principle:

$$P = \frac{W}{t} = p * \dot{V}$$

(P – cardiac power, W – mechanical work, t - time, p – arterial pressure, $\Delta\dot{V}$ – cardiac output).

The arterial pressure equals the afterload which is maintained at 100 cmH₂O constantly. Cardiac output was calculated by addition of aortic and coronary flow (Doenst et al. 1998, Doenst et al. 1999). Thus, the equation simplifies to

$$P = \frac{\dot{V}_{aortic} + \dot{V}_{coronary}}{6.12}$$

(P – cardiac power [mW], \dot{V}_{aortic} – aortic flow [ml/min], $\dot{V}_{coronary}$ – coronary flow [ml/min], 6.12 – correction factor accounting for the constant arterial pressure and unit conversions [m²/N]).

4.2.3 Perfusion protocol

Hearts were perfused for 60 min with Krebs-Henseleit buffer containing glucose (5 mM) and sodium oleate (0.4 mM) bound to 1% BSA. After an initial phase of perfusion to ensure stabile mechanical function, 60 µl of [U-¹⁴C]-glucose and 5 µl of [9,10-³H]-oleate were added to the perfusion system to start the experiment. Beginning at t = 0 min, 2 ml aliquots of perfusion medium were withdrawn for later determination of glucose and fatty acid oxidation every 5 min. Similarly, the gaseous ¹⁴C-CO₂ derived from glucose oxidation was collected in 5 min intervals by trapping in benzethonium hydroxide. After 30 min, insulin (0.5 IU/l) was added to the perfusion medium. Thus, the first 30 min of the experiment provided information

about the basal cardiac substrate oxidation. The second half of the perfusion protocol were dedicated to investigate insulin stimulated metabolic conditions. Figure 6 illustrates the applied protocol. At the end of the perfusion, hearts were frozen in liquid nitrogen for further analysis.

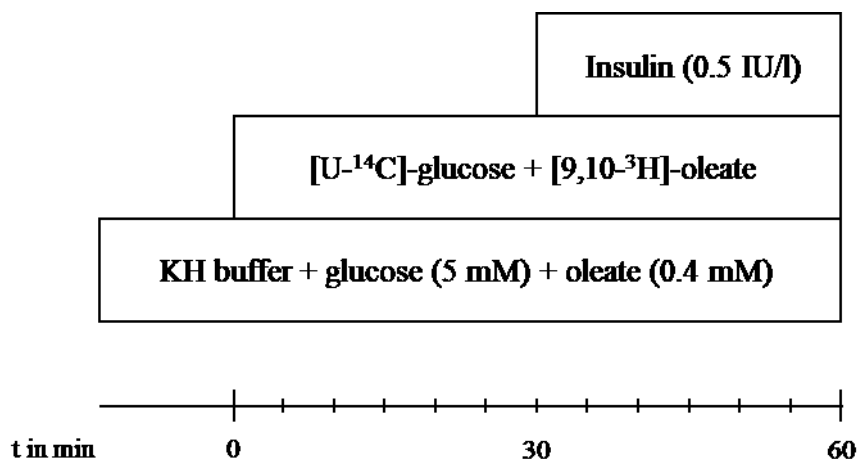


Figure 6: Perfusion protocol. After an initial phase allowing functional stabilization, labeled substrates were administered to examine cardiac metabolism under basal conditions. At t = 30 min, insulin was added to investigate cardiac metabolism after stimulation. KH buffer – Krebs-Henseleit buffer.

4.3 Radioisotopic techniques

4.3.1 Determination of glucose oxidation

The oxidation of [U-¹⁴C]-glucose by pyruvate dehydrogenase and the citric acid cycle during the isolated working heart perfusion leads to a release of ¹⁴CO₂. The measurement of ¹⁴CO₂ at consecutive time points of the perfusion protocol combined with knowledge about the total specific activity of the system allows the estimation of glucose oxidation in absolute values. The whole perfusion system was rendered gas tight and the gaseous ¹⁴CO₂ was channeled into a scintillation vial containing 5 ml of benzethonium hydroxide solution (333 mM, diluted with methanol) which is able to bind ¹⁴CO₂. After addition of 5 ml of scintillation cocktail, the samples were mixed and activity was measured using a liquid scintillation counter.

To determine the amount of ¹⁴CO₂ solved in the perfusion, a scintillation vial was prepared with 1 ml of benzethonium hydroxide solution for each sample. 0.5 ml of sample drawn from

the perfusion system were transferred into a 1.5 ml tube which was cautiously placed inside the scintillation vial without spilling any of the content. The vial was sealed gas tight with a rubber plug. 0.1 ml of perchloric acid were injected into the sample through the plug without compromising the seal. The acidification of the sample promotes the shift of $^{14}\text{CO}_2$ from the aqueous to the gaseous phase and enables the binding to benzethonium hydroxide. After incubation for 12 h on a shaker adjusted to medium speed, the rubber plug and the 1.5 ml tube containing the sample were carefully removed. Finally, 4 ml of scintillation cocktail were added to the scintillation vial and activity was measured using a liquid scintillation counter after mixing. Combination of the activity determined in the aqueous and gaseous phase allows the calculation of total glucose oxidation:

$$GO = \frac{\Delta(A_{\text{aqueous}} + A_{\text{gaseous}})}{A_{\text{spez}} * m_{\text{dry}}}$$

(GO – glucose oxidation [$\mu\text{mol}/\text{min}/\text{g}$ dry weight], ΔA – shift in activity over time [cpm/min], A_{spez} – specific activity of the medium [cpm/ μmol glucose], m_{dry} – cardiac dry weight [g]).

The complete aerobic oxidation of 1 mol of glucose generates 4 mol of ATP, 10 mol of NADH and 2 mol of FADH_2 . Assuming an ATP yield of 2.5 mol ATP/NADH and 1.5 mol ATP/ FADH_2 (Hinkle 2005), the breakdown of 1 mol of glucose generates a total of 32 mol of ATP. Thus, ATP production derived from GO was calculated as $\text{GO} [\mu\text{mol}/\text{min}/\text{g}$ dry weight] * 32.

4.3.2 Determination of fatty acid oxidation

During the breakdown of $[9,10\text{-}^3\text{H}]\text{-oleate}$ by beta-oxidation, ^3H -labeled water is liberated. The measurement of $^3\text{H}_2\text{O}$ at consecutive time points of the perfusion protocol combined with knowledge about the total specific activity of the system allows the estimation of beta-oxidation in absolute values. Samples of the perfusion medium were obtained every 5 min. To quantify $^3\text{H}_2\text{O}$, the labeled water was separated from all other radioactive molecules in the medium. Filter columns were made by preparation of 1 ml syringes with glass fiber pads and 0.5 ml of a filter resin. The columns were washed with 0.5 ml of water twice. Then, 0.1 ml of sample were added followed by two further elution steps with 0.1 ml and 0.7 ml of water,

respectively. The elute was saved in a scintillation vial. After addition of 3 ml of scintillation cocktail, the samples were vortexed.

To determine the total specific activity of the perfusion medium, 0.1 ml of three different samples were mixed with 3 ml of scintillation cocktail without prior filtration. Finally, the activity of all prepared samples was determined using a liquid scintillation counter. Oleic acid oxidation was calculated as:

$$FAO = \frac{\Delta A}{A_{spez} * m_{dry}}$$

(FAO – fatty acid oxidation [$\mu\text{mol}/\text{min}/\text{g}$ dry weight], ΔA – shift in activity over time [cpm], A_{spez} – specific activity of the medium [cpm/ μmol oleic acid], m_{dry} – cardiac dry weight [g]).

The complete breakdown of 1 mol of oleic acid by beta-oxidation generates 9 mol of acetyl-CoA, 8 mol of NADH and 7 mol of FADH_2 . The oxidation of 9 mol of acetyl-CoA in the citric acid cycle yields 9 mol of ATP, 27 mol of NADH and 9 mol of FADH_2 . Assuming an ATP yield of 2.5 mol ATP/NADH and 1.5 mol ATP/ FADH_2 (Hinkle 2005), the oxidation of 1 mol of oleic acid generates a total of 120.5 mol of ATP. Since 2 ATP are required to activate oleic acid to oleyl-CoA at the beginning of beta-oxidation, the net ATP production equals 118.5 mol of ATP. Thus, ATP production derived from FAO was calculated as $\text{FAO} [\mu\text{mol}/\text{min}/\text{g dry weight}] * 118.5$.

4.4 Tissue chemistry and photometric methods

4.4.1 Carnitine palmitoyltransferase I/II activity

Carnitine palmitoyltransferase I and II (CPT I and CPT II) activities were measured in cardiac extracts as described previously with some modifications (Bieber et al. 1972). The fusion of L-carnitine and palmitoyl-CoA to palmitoylcarnitine catalyzed by CPT I and CPT II liberates Coenzyme A which reacts with 5,5'-dithiobis-2-nitrobenzoic acid (DTNB) stoichiometrically to produce mercaptide anions. The generated mercaptide anions were detected spectrophotometrically at 412 nm. To distinguish between CPT I and CPT II activity,

malonyl-CoA was added to the reaction mix after total CPT activity was determined. The difference of total CPT activity and CPT activity after inhibition equals the CPT II activity. 20 mg of powdered cardiac tissue were homogenized in 200 μ l of extraction puffer (40 mM HEPES, 1 mM EDTA, 2 mM $MgCl_2$, pH=7.4) for 1 min using a Teflon homogenizer at 1000 rpm. Next, each sample was sonicated three times for 10 s (7 cycles, 70% power). 2 μ l of 5% Triton-100 were added and the homogenates were incubated for 5 min on ice after mixing. Finally, the samples were centrifuged at 12000 rcf for 5 min at 4°C. The supernatants were saved and assayed for CPT activity. 5 μ l of undiluted sample were incubated with 185 μ l of reaction puffer (34 mM HEPES, 99 mM Tris-Cl, 0.08% Triton-100, 1.28 mM EDTA, 1.35 mM L-carnitine, 0.27 mM DTNB) for 3 min at 25°C. Hereafter, 10 μ l of 0.7 mM palmitoyl-CoA or water were added to start the reaction or as control, respectively. The change of absorbance at 412 nm was measured continuously for 8 min before 10 μ l of 0.21 mM malonyl-CoA were added to measure the CPT II activity exclusively. Enzymatic activity was calculated based on the law of Lambert-Beer ($\epsilon_{DTNB} = 13.9 \text{ mM}^{-1}\text{cm}^{-1}$) and normalized to cardiac protein concentration. Each sample was measured as triplicate.

4.4.2 Bradford protein assay

Protein concentrations of cardiac extracts were measured using the method developed by Bradford (Bradford 1976). After binding to protein, the dye Coomassie Brilliant Blue G-250 contained in the reaction mix changes its color to blue and is detected spectrophotometrically at 595nm. Cardiac extracts were diluted 20-fold. The Protein Assay Dye Reagent provided by Bio-Rad was diluted 5-fold. 5 μ l of sample were mixed with 200 μ l of the diluted dye. After incubation for 3 min at room temperature, the absorbance at 595 nm was measured with a Synergy 2 Multi-Mode Microplate Reader (BioTek Instruments). Protein concentrations were calculated based on a standard curve derived from a freshly prepared BSA protein standard. All samples were measured as triplicates.

4.4.3 Cardiac dry weight

Cardiac power, glucose oxidation and fatty acid oxidation were normalized to cardiac dry weight. About 100 mg of powdered heart sample were incubated for 48 h at 72°C to evaporate any water present. Hereafter, the weight of each sample was recorded and the obtained wet-dry ratio was used to calculate cardiac dry weight.

4.5 Statistical analysis

Comparison of means was performed using two-way analysis of variance (two-way ANOVA) and Tukey post hoc test (Prism 7, GraphPad software, Inc.). Differences of means with a p-value lower than 0.05 were considered statistically significant. Results are presented as mean \pm standard error of the mean.

5 Results

5.1 Morphology

Body, heart, liver and lung weights of all animals were recorded during the perfusion experiment (Figure 7a-d). Animals bred for low intrinsic running capacity (LCR) presented with a significantly increased body weight compared to rats with high intrinsic running capacity (HCR) at all time points investigated. Heart weights tended to be slightly higher in LCR than HCR without reaching statistical significance. Lung weights were equal for all groups. Liver weights of LCR control rats were increased compared to HCR but did not differ significantly in the remaining groups. The observed increase of body weight in LCR is mainly due to enlarged peripheral and visceral adipose tissue depots (not shown).

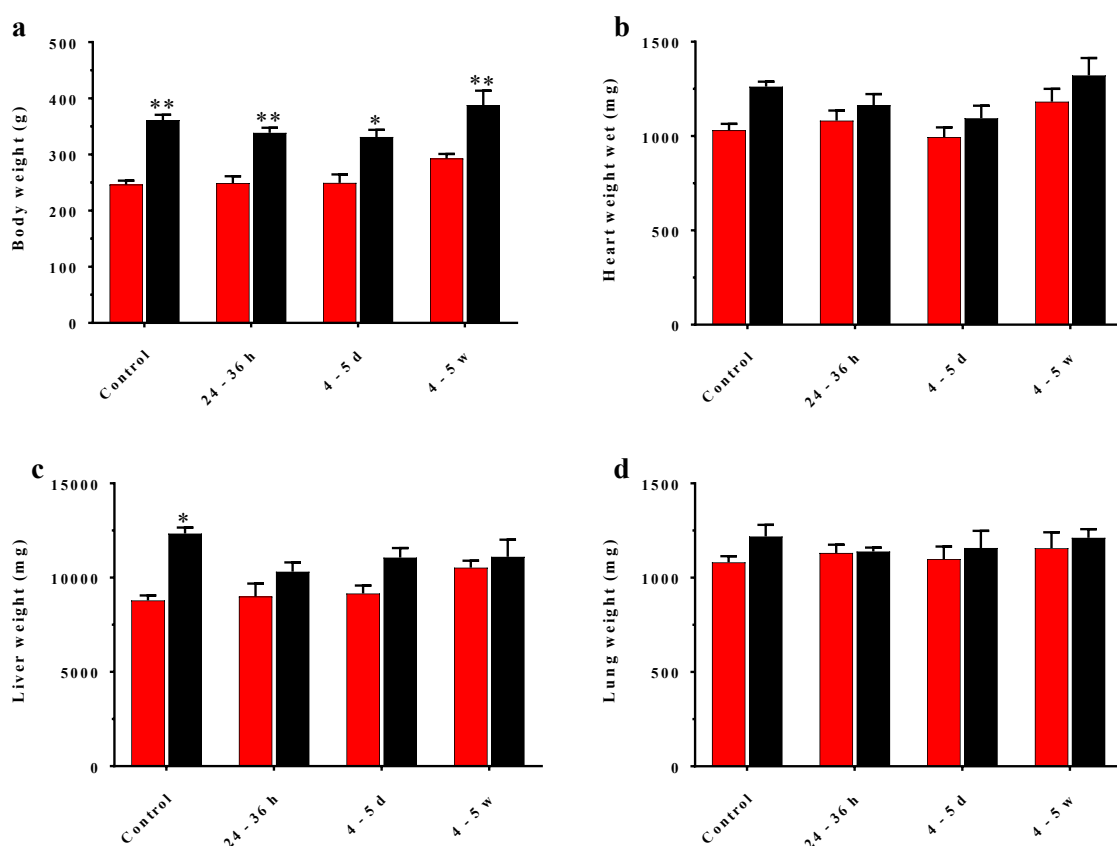


Figure 7: Morphological parameters. Body weight (a), heart weight wet (b), liver weight (c) and lung weight (d) of high capacity runners (HCR, ■) and low capacity runners (LCR, ■) at different time points after sepsis induction compared to control. $n = 4$ for HCR 4-5 d and HCR 4-5 w, $n = 7-8$ for the remaining groups. Data presented as mean \pm standard error of the mean. * - $p < 0.05$, ** - $p < 0.01$.

5.2 Cardiac power

Cardiac performance parameters have been monitored continuously during isolated working heart perfusions using a pressure transducer connected to the perfusion system. Every 5 min, cardiac power was assessed and recorded (Figure 8). Baseline cardiac power, measured during the first span of the perfusion, did not differ significantly between LCR and HCR rats. Administration of insulin did not lead to relevant changes of cardiac function. In HCR, cardiac power tended to be decreased 4-5 w after sepsis induction compared to control without reaching statistical significance. Sepsis induction did not compromise cardiac performance after short-term (24-36 w).

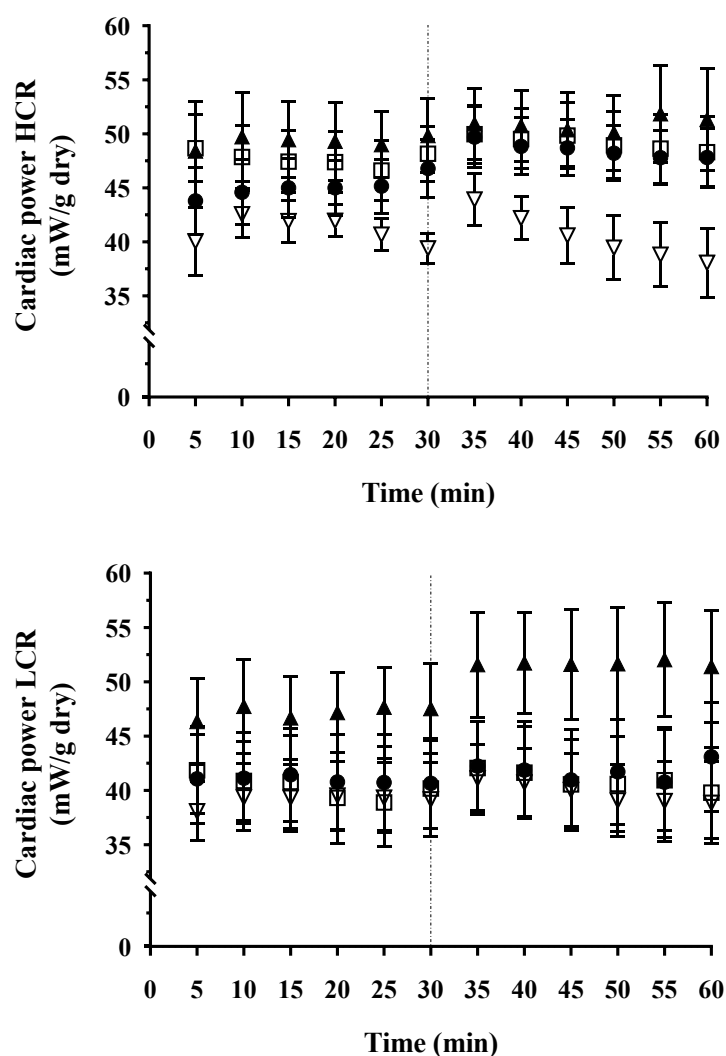


Figure 8: Cardiac power of HCR and LCR hearts over time. Cardiac power normalized to cardiac dry weight of high capacity runners (HCR) and low capacity runners (LCR) 24-36 h (□), 4-5 d (▲) and 4-5 w (▽) after sepsis induction and control (●). Vertical line at t = 30 min indicates administration of insulin. n = 4 for HCR 4-5 d and HCR 4-5 w, n = 7-8 for the remaining groups. Data presented as mean \pm standard error of the mean.

5.3 Cardiac performance parameters

Besides cardiac power, heart rate as well as cardiac contractility were recorded continuously. Since administration of insulin did neither affect heart rate nor contractility, the presented data represent values averaged over 60 min of perfusion (Figure 9a-c). Similar to cardiac power, heart rate was not dependent on intrinsic exercise capacity. Furthermore, sepsis induction did not provoke any significant changes in heart rate *ex vivo*. Cardiac contractility tended to be higher both in HCR and LCR 4-5 d after sepsis induction compared to control without reaching statistical significance. Taken together, induction of sepsis did not affect cardiac mechanical function of isolated working hearts at any given timepoint.

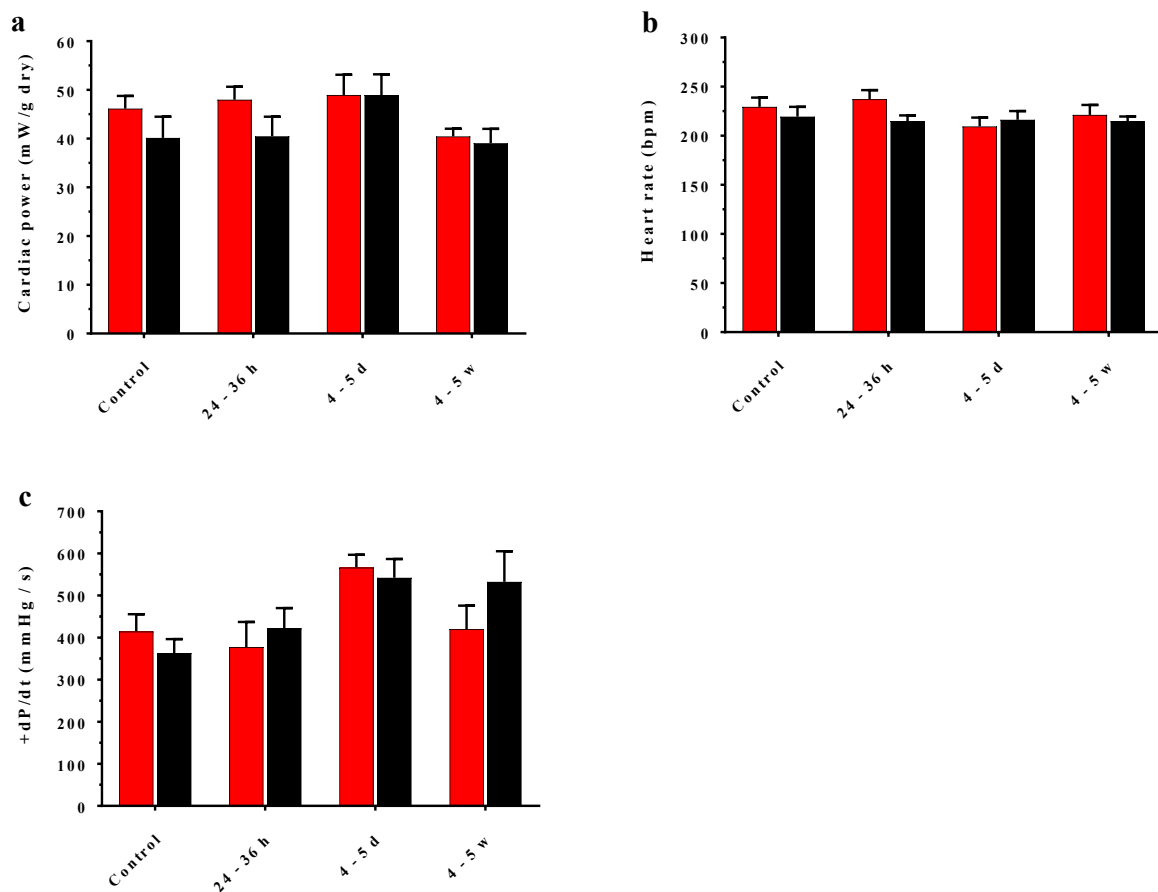


Figure 9: Cardiac performance assessed during isolated working heart perfusions. Cardiac power averaged over 60 min (a), heart rate (b) and peak ventricular contractility (+dP/dt, c) of high capacity runners (HCR, ■) and low capacity runners (LCR, ■) at different time points after sepsis induction compared to control. $n = 4$ for HCR 4-5 d and HCR 4-5 w, $n = 7-8$ for the remaining groups. Data presented as mean \pm standard error of the mean.

5.4 Baseline cardiac glucose oxidation

Cardiac baseline glucose oxidation (GO) was determined based on samples taken from the perfusion medium during the first span of the perfusion before administration of insulin. Baseline GO tended to be higher in LCR hearts compared to HCR hearts at all investigated timepoints (Figure 10). Aerobic glucose utilization appeared to be lowest 24-36 h after sepsis induction in HCR as well as LCR. On the other end, baseline GO was highest 4-5 d after induction of sepsis in both strains. However, all changes did not reach statistical significance compared to control.

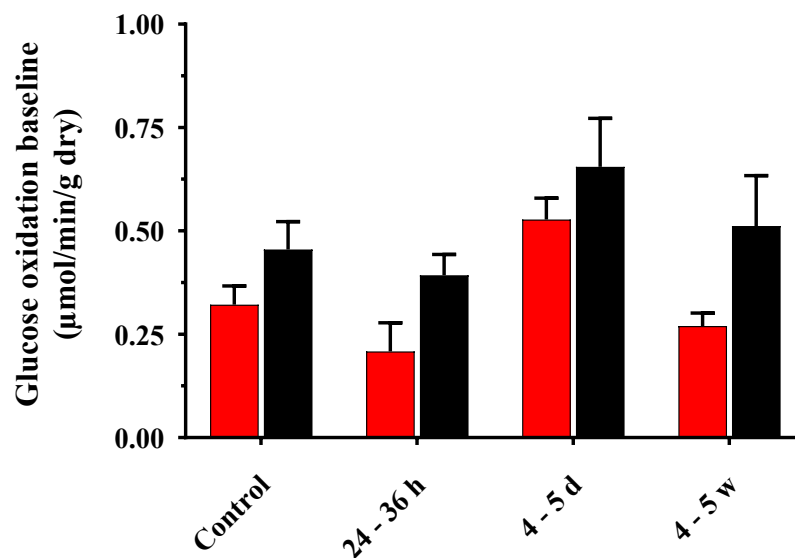


Figure 10: Baseline cardiac glucose oxidation. Glucose oxidation of high capacity runners (HCR, ■) and low capacity runners (LCR, ■) before administration of insulin at different time points after sepsis induction compared to control. $n = 4$ for HCR 4-5 d and HCR 4-5 w, $n = 5$ for LCR 4-5 w, $n = 6-8$ for the remaining groups. Data presented as mean \pm standard error of the mean.

5.5 Insulin stimulated cardiac glucose oxidation

Insulin stimulated cardiac GO was determined based on samples taken from the perfusion medium during the second span of the perfusion after administration of insulin. Administration of insulin caused a robust increase of oxidative glucose metabolism in all investigated groups (Figure 11a-b). The tendency of increased GO in LCR hearts compared to HCR hearts observed at baseline conditions remained after insulin stimulation. The absolute change of GO was comparable for all groups independent of intrinsic exercise capacity and timepoint after sepsis induction. The results suggest preserved cardiac insulin sensitivity during acute sepsis and in sepsis survivors.

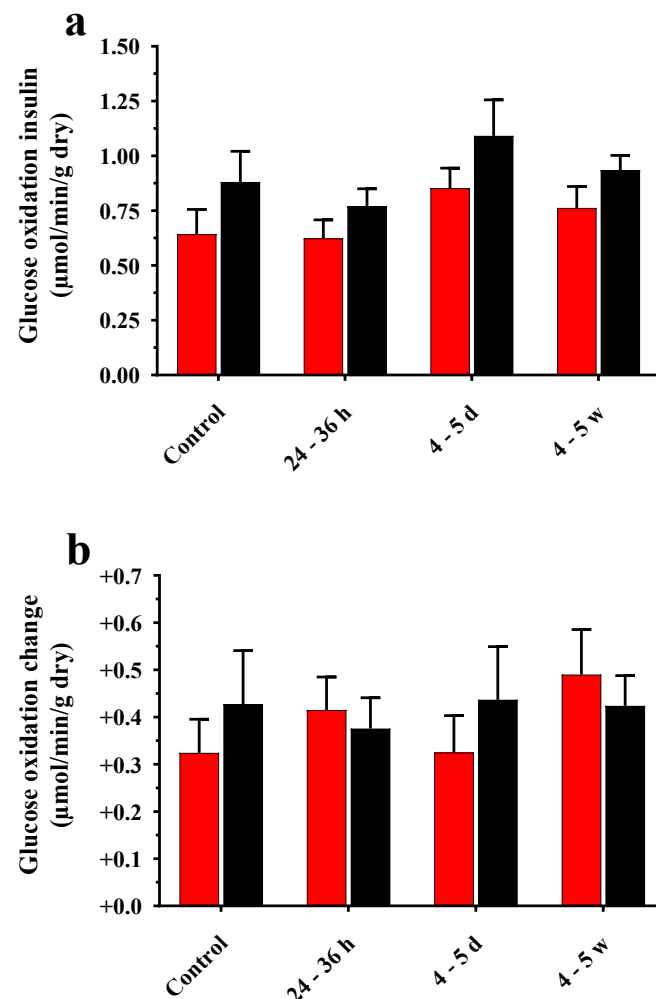


Figure 11: Cardiac glucose oxidation after administration of insulin. Insulin stimulated glucose oxidation (a) and change of glucose oxidation calculated as insulin stimulated minus baseline glucose oxidation (b) of high capacity runners (HCR, ■) and low capacity runners (LCR, ■) at different time points after sepsis induction compared to control $n = 4$ for HCR 4-5 d and HCR 4-5 w, $n = 5$ for LCR 4-5 w, $n = 6-8$ for the remaining groups. Data presented as mean \pm standard error of the mean.

5.6 Baseline cardiac fatty acid oxidation

Cardiac baseline fatty acid oxidation (FAO) was determined based on samples taken from the perfusion medium during the first span of the perfusion before administration of insulin. While GO was found to be higher in LCR than HCR, FAO tended to be reduced in LCR compared to HCR except for hearts perfused 4-5 w after sepsis induction (Figure 12). Baseline FAO was highest 4-5 d after induction of sepsis in HCR hearts. The lowest rate of FAO was observed in LCR hearts 24-36 h after sepsis induction. All changes in FAO failed to reach statistical significance compared to control, indicating that baseline FAO is not altered during acute sepsis and in sepsis survivors.

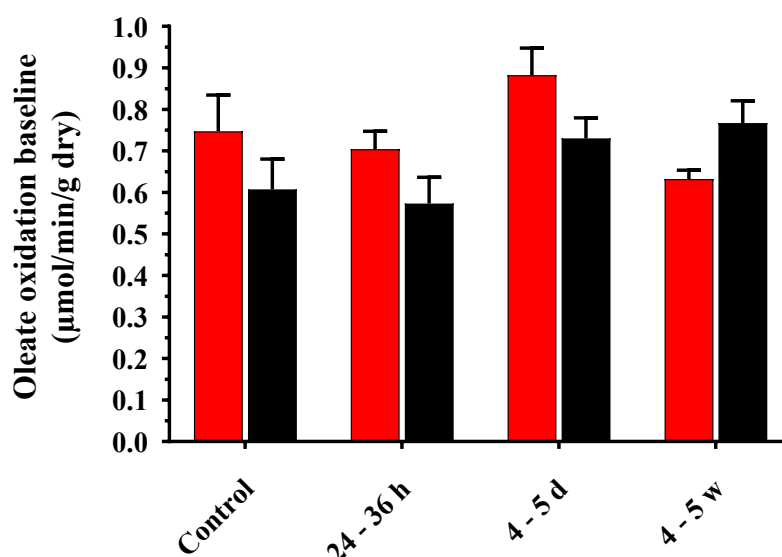


Figure 12: Baseline cardiac fatty acid oxidation. Baseline fatty acid oxidation of high capacity runners (HCR, ■) and low capacity runners (LCR, ■) at different time points after sepsis induction compared to control. $n = 4$ for HCR 4-5 d and HCR 4-5 w, $n = 6-8$ for the remaining groups. Data presented as mean \pm standard error of the mean.

5.7 Insulin stimulated cardiac fatty acid oxidation

Administration of insulin provoked a reduction of FAO in all groups. The tendency of higher rates of FAO in HCR hearts relative to LCR hearts was maintained after stimulation with insulin (Figure 13). Only 4-5 w after sepsis induction, LCR appeared to oxidize more fat than HCR. The absolute change of FAO after insulin stimulation was not significantly different between groups. However, the decline of FAO was most pronounced 4-5 w after sepsis induction in both HCR and LCR. These findings represent further evidence for uncompromised cardiac insulin sensitivity during sepsis and in sepsis survivors.

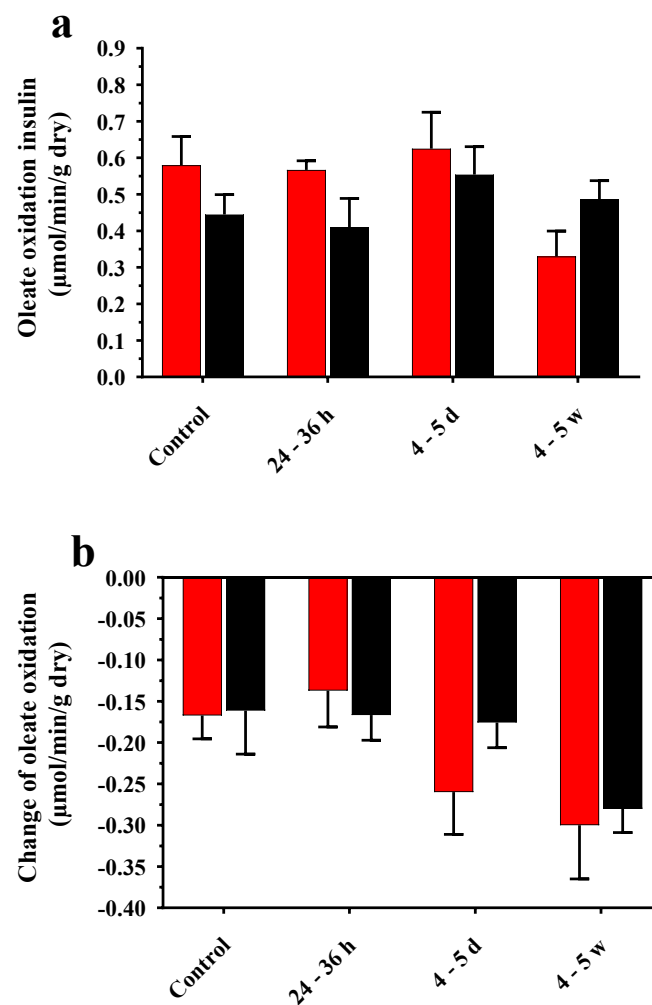


Figure 13: Cardiac fatty acid oxidation after administration of insulin. Insulin stimulated fatty acid oxidation (a) and change of fatty acid oxidation calculated as insulin stimulated minus baseline fatty acid (b) of high capacity runners (HCR, ■) and low capacity runners (LCR, ■) at different time points after sepsis induction compared to control. $n = 4$ for HCR 4-5 d and HCR 4-5 w, $n = 6-8$ for the remaining groups. Data presented as mean \pm standard error of the mean.

5.8 Ratio of glucose oxidation to fatty acid oxidation

The ratio of glucose oxidation to fatty acid oxidation (GO/FAO) was calculated to visualize cardiac substrate preference and selection (Figure 14a-b). At baseline conditions, GO/FAO was higher in all LCR groups compared to the corresponding HCR groups, emphasizing that LCR hearts rely more on oxidative glucose metabolism than HCR hearts. Administration of insulin caused a substantial increase of GO/FAO in all investigated groups. This illustrated an adequate response to insulin stimulation independent of intrinsic exercise capacity. Acute sepsis or sepsis survival did not appear to impair cardiac insulin sensitivity in our experimental model.

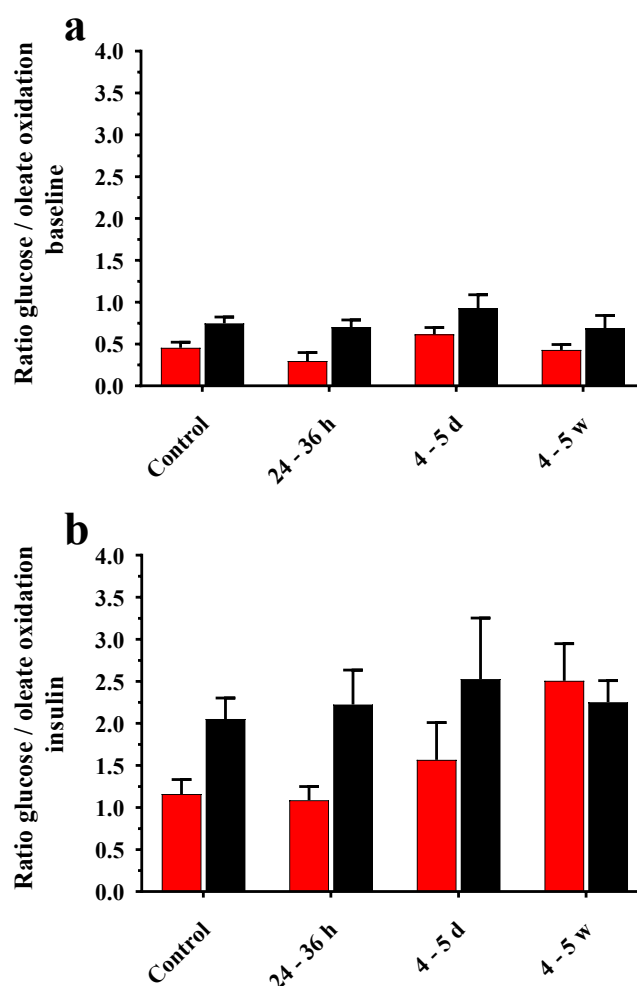


Figure 14: Ratio of glucose oxidation to fatty acid oxidation. Ratio of cardiac glucose oxidation to fatty acid oxidation before (a) and after (b) administration of insulin of high capacity runners (HCR, ■) and low capacity runners (LCR, ■) at different time points after sepsis induction compared to control. n = 4 for HCR 4-5 d and HCR 4-5 w, n = 5 for LCR 24-36 h and LCR 4-5 w, n = 6-8 for the remaining groups. Data presented as mean ± standard error of the mean.

5.9 Cardiac efficiency

The efficiency of cardiac performance can be described based on the ratio of ATP production to cardiac power (Figure 15a-b). Under baseline conditions, HCR and LCR hearts produced comparable amounts of ATP per milliwatt of cardiac power. Cardiac efficiency tended to be slightly higher 24-36 h after sepsis induction in both HCR and LCR. Sepsis survivors did not present with any changes of cardiac efficiency compared to control. The ratio of ATP production to cardiac power decreased slightly in all groups but LCR control upon insulin administration, indicating improved efficiency of insulin stimulated cardiac function. However, all effects failed to reach statistical significance.

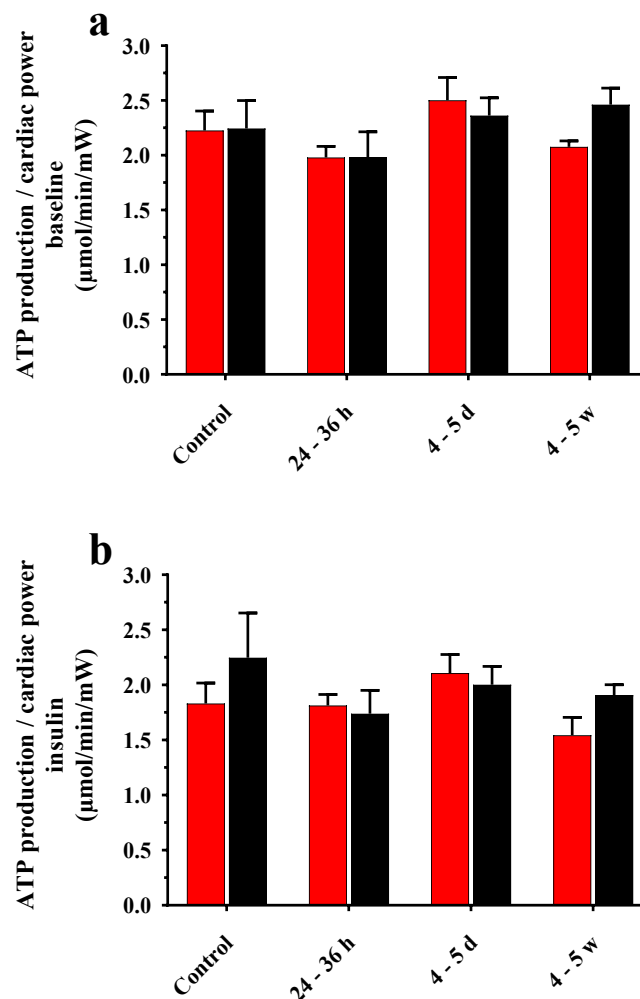


Figure 15: Cardiac efficiency expressed as ratio of ATP production to cardiac power. Ratios of ATP production to cardiac power before (a) and after (b) insulin stimulation of high capacity runners (HCR, ■) and low capacity runners (LCR, ■) at different time points after sepsis induction compared to control. $n = 4$ for HCR 4-5 d and HCR 4-5 w, $n = 5$ for LCR 24-36 h and LCR 4-5 w, $n = 6-8$ for the remaining groups. Data presented as mean \pm standard error of the mean.

5.10 Carnitine palmitoyltransferase I and II activity

Carnitine palmitoyltransferase I (CPT I) and II (CPT II) activities of insulin stimulated cardiac samples were determined before and 24 h after sepsis induction (Figure 16). Total CPT activity was neither affected by the genetic predisposition for exercise capacity nor by the induction of sepsis. CPT I inhibition by malonyl-CoA provoked a comparable decline of enzymatic activity in all groups, indicating similar CPT I and CPT II activities in all examined samples.

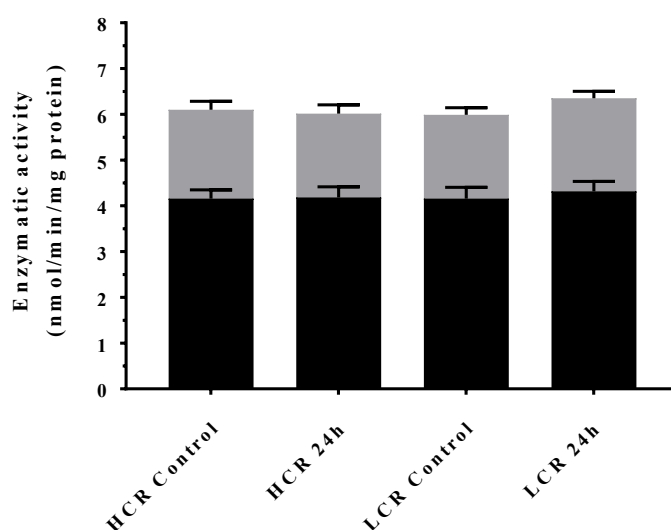


Figure 16: Cardiac CPT I and II activities. Cardiac carnitine palmitoyltransferase I (CPT I, ■) and II (CPT II, ■) activities of high capacity runners (HCR) and low capacity runners (LCR) 24 h after sepsis induction compared to control. n = 4-7. Data presented as mean \pm standard error of the mean.

6 Discussion

The current study is the first to investigate septic effects on cardiac metabolism and function in dependence of intrinsic exercise capacity. Basal cardiac substrate oxidation was not substantially altered during sepsis or in sepsis-survivors. Cardiac insulin sensitivity appeared to be preserved at all investigated time points. Cardiac function assessed *ex vivo* during isolated working heart perfusions was not compromised in acute sepsis or in sepsis-survivors. Intrinsic exercise capacity did not influence cardiac metabolism or function in septic animals significantly.

Basal glucose and fatty acid oxidation were not changed 24-36 h after sepsis induction or in sepsis survivors. Indeed, this finding is in line with the few studies focusing on cardiac substrate metabolism in sepsis previously. In male Sprague-Dawley rats, sepsis was induced by cecal ligation and puncture (CLP) followed by isolated working heart perfusions 12 - 14 h later (Watts et al. 2004). Glucose oxidation, determined by measuring $^{14}\text{CO}_2$ liberated from $[\text{U-}^{14}\text{C}]$ -glucose, and oxygen consumption did not differ between septic hearts and control. However, cardiac efficiency was decreased since septic hearts displayed reduced cardiac function. Another group induced sepsis in rats by inoculation of a pooled fecal homogenate and performed Langendorff perfusions with medium containing ^{14}C -labeled glucose, lactate or palmitate 48 h later to assess cardiac substrate oxidation (McDonough et al. 1986). The contribution of the three substrates to oxidative ATP formation was comparable in hearts from septic and control animals, indicating an unchanged myocardial substrate preference. Lastly, endotoxemia was provoked in male Sprague-Dawley rats by intraperitoneal administration of lipopolysaccharides (LPS) and isolated working heart perfusions were performed 6 h later (Soraya et al. 2016). Glucose metabolism including rates of glucose uptake, glycogen synthesis, glycolysis and glucose oxidation were not affected in endotoxemic hearts. Interestingly, palmitate oxidation was reduced in endotoxemic hearts, proportional to an observed decline in left ventricular function. Thus, unchanged cardiac substrate utilization was found in the majority of investigated septic rat models and is supported by our results. Intrinsic exercise capacity did not affect cardiac baseline metabolism markedly, independent of the timepoint after sepsis induction. However, low capacity runner (LCR) hearts appeared to oxidize slightly more glucose than high capacity runner (HCR) hearts. Correspondingly,

fatty acid oxidation seemed to be lower in LCR compared to HCR. These patterns of substrate preference have not been reported as pronounced in previous sets of HCR and LCR heart perfusions (Schwarzer et al. 2010). Here, rates of glucose oxidation were similar for the two populations, only fatty acid oxidation appeared slightly lower in LCR compared to HCR. Of course, the trends found in the present study may be purely coincidental since the differences in glucose and fatty acid oxidation failed to reach statistical significance. However, a recent proteomic analysis of HCR and LCR hearts advocated for a possible divergence in substrate selection (Burniston et al. 2011). Interestingly, HCR hearts exhibited significant increases of enzymes involved in β -oxidation compared to LCR, including short-chain specific acyl-CoA dehydrogenase, enoyl-CoA hydratase and hydroxyacyl-CoA dehydrogenase. Comparable observations were made on transcriptional level before (Bye et al. 2008). Expression of genes encoding enzymes involved in oxidative fatty acid utilization was up-regulated in hearts of HCR rats. Moreover, LCR rats expressed higher amounts of genes participating in cardiac glucose metabolism. Hence, the tendency of LCR hearts to oxidize more glucose and less fatty acids compared to HCR seen in the present study may be more than just coincidence.

Beside basal cardiac metabolism, this study also addressed cardiac insulin sensitivity. All hearts challenged with insulin during isolated heart perfusions responded with robust increases in glucose oxidation and corresponding decreases in fatty acid oxidation, indicating preserved insulin sensitivity. Neither acute sepsis nor sepsis-survival influenced cardiac insulin sensitivity. At first glance, this appears surprising because sepsis was associated with the development of insulin resistance (IR) before (Marik und Raghavan 2004, Chambrier et al. 2000, Agwunobi et al. 2000, Illuri et al. 2016). The mediation of IR in septic conditions was mainly attributed to players of the proinflammatory cascade activated during sepsis, such as tumor necrosis factor alpha (TNF- α) and interleukin 1, or to the action of endotoxins directly. However, cytokine and endotoxin mediated effects on the insulin signaling cascade were predominantly observed in hepatocytes or peripheral tissues including skeletal muscle and adipose tissue but less in cardiomyocytes (Bierbrauer und Weber-Carstens 2011). In one study, LPS were administered intravenously for 74 h in Sprague-Dawley rats to induce prolonged endotoxemia (McCowen et al. 2001). Insulin-stimulated tyrosine phosphorylation of insulin receptors, insulin receptor substrate (IRS) 1 and -2 and binding of the p85 subunit of phosphatidylinositol 3-kinase to IRS-1 were significantly reduced in liver and skeletal muscle, demonstrating deficits in early steps of insulin signaling upon endotoxemic challenge. In cultured adipocytes, TNF- α treatment provoked an increase of serine phosphorylation of

IRS-1 (Hotamisligil et al. 1996). Serine phosphorylation of IRS-1 interferes with the insulin-stimulated tyrosine phosphorylation of IRS-1 and confers IR. Thus, one must differentiate between systemic and cardiac IR assessed in isolated hearts. The presence of systemic resistance does not automatically guarantee IR in distinct organs such as the heart. The results of the present study suggest that cardiac insulin sensitivity is not compromised within the framework of the applied model of sepsis. Testing for systemic insulin sensitivity was not within the scope of this project. In perspective, it would be of great interest if our septic animal model is characterized by dissociated, organ-specific IR.

Intrinsic exercise capacity did not affect cardiac insulin sensitivity in the present study. The responses of both HCR and LCR hearts to insulin stimulation were comparable independent of sepsis or sepsis-survival. This finding is in line with previous experiments. In healthy 21 week old HCR and LCR rats, cardiac sensitivity to insulin assessed during isolated working heart perfusions was indifferent (Schwarzer et al. 2010). The response to insulin measured as increase in glucose oxidation was more pronounced in their set of experiments compared to our results (Δ glucose oxidation: $+0.59 \mu\text{mol}/\text{min}/\text{g}$ dry weight vs $+0.39 \mu\text{mol}/\text{min}/\text{g}$ dry weight). However, this may be simply explained by different dosages of insulin used in the studies (1 IU/l vs 0.5 IU/l, respectively). Interestingly, low intrinsic exercise capacity was associated to systemic IR before (Morris et al. 2009, Noland et al. 2007). Fasting glucose and serum insulin levels were significantly higher in LCR rats, indicative of reduced sensitivity to insulin (Schwarzer et al. 2010, Wisloff et al. 2005). This is yet another example for the presence of dissociated IR that hints on different mechanisms contributing to cardiac IR on the one hand and peripheral IR on the other.

Administration of insulin caused a tendential decrease of the ratio of ATP production to cardiac power in the majority of groups, hinting on improved cardiac efficiency. This observation is in line with previous findings. In perfusion experiments of HCR and LCR hearts, insulin increased cardiac efficiency in both strains (Schwarzer et al. 2010). In general, insulin signaling and the concomitant shift from fatty acid oxidation towards glucose utilization is considered to decrease cardiac oxygen consumption, reduce mitochondrial uncoupling and therefore favor energetic efficiency (Iliadis et al. 2011, Boudina et al. 2007). Cardiac efficiency was not disturbed in acute sepsis or in sepsis survivors. While somewhat surprising, preserved cardiac efficiency fits well into the overall picture of our model, considering the unaffected substrate metabolism, insulin sensitivity and cardiac function in septic and post-septic animals.

Cardiac function assessed *ex vivo* during isolated working heart perfusions was not compromised 24-36 h after induction of sepsis or in sepsis survivors independent of intrinsic exercise capacity. Cardiac power, heart rate and peak ventricular contractility were comparable between all groups. Of course, *ex vivo* cardiac function does not necessarily reflect the *in vivo* situation. Maintained cardiac performance of isolated working hearts primarily demonstrates structural integrity of the heart and hints on the absence of static myocardial damage. *In vivo*, a plethora of factors can influence cardiac mechanical function and potentially cause dynamic heart failure. In the context of sepsis, potential cardiodepressive effects of inflammatory mediators, such as cytokines or endotoxins, come to mind first. When the heart is removed from the inflammatory milieu of sepsis for heart perfusions, these influences disappear and cardiac function may normalize. However, we do not have evidence that *in vivo* cardiac performance was compromised in our model of sepsis induced by peritoneal contamination and infection (PCI). Echocardiography performed in HCR and LCR rats 6 h and 24 h after sepsis induction did not reveal significant reduction of cardiac function. This was unexpected since previous studies observed cardiac dysfunction after employing the PCI model in a different rat species. In male Wistar rats, sepsis induced by PCI provoked decreases of stroke volume, end-diastolic volume and cardiac output measured with echocardiography after 6 h (Dyson et al. 2011). After 24 h, these effects were still present but to a lesser extent. Importantly, only a subset of rats (55%) was affected by cardiac impairment. The remaining animals presented with normal cardiac function or alleviated symptoms. Decline in cardiac function was associated to a worse prognosis and reduction of stroke volume was determined a robust predictor of outcome (Rudiger et al. 2013). The PCI model of sepsis had never been applied on HCR and LCR rats before. For unknown reasons, the impairment of cardiac function seen in Wistar rats after PCI was not reproduced in HCR and LCR strains despite inducing critical illness (assessed using the clinical severity score) and causing comparable mortality.

Other studies using a more popular model of systemic inflammation and endotoxemia observed even more pronounced disturbances of cardiac function both *in vivo* and *ex vivo*. For instance, intraperitoneal LPS injection (10 m/kg) in mice caused a significant reduction of cardiac contractility 3 h, 12 h and 24 h after injection (Umbarawan et al. 2017). In Wistar rats, intravenous administration of LPS (15 mg/kg) prompted a significant decline of mean arterial pressure and peak ventricular contractility after 2 h already (Yang et al. 2018). Sprague-Dawley rats reacted with profound decreases of ejection fraction and fractional shortening to an intraperitoneal LPS (15 mg/kg) challenge, indicating impaired left ventricular function

(Unuma et al. 2018). However, direct comparisons of the LPS/endotoxemia models of sepsis and PCI are problematic as they differ in several points. LPS treatment caused significant higher TNF- α levels, responses to oxidative stress and degree of cell death than polymicrobial sepsis induced by PCI (Recknagel et al. 2013). A drawback of rodent LPS models is the amount of LPS used in the respective experiments. The LD50 dose of LPS in mice was found to be about 1000-fold to 10000-fold greater than the dose required to provoke critical septic illness in humans (Fink 2014). For that and other reasons, the LPS model has been doubted to properly replicate the pathophysiology and pathomechanisms of sepsis (Rittirsch et al. 2007). In contrast, PCI appeared to mimic many features characteristic for human sepsis, such as coagulation abnormalities, liver dysfunction, microcirculatory defects and concomitant multi-organ failure (Gonnert et al. 2011). Therefore, LPS models and PCI differ in various properties and a comparison of respective observations including cardiac dysfunction are only possible to a limited extent.

Another example of model-dependent effects may be the alteration of CPT activity. We did not detect any changes in cardiac CPT activity related to sepsis. Both CPT I and II activities measured in septic hearts 24 h after fecal injection were similar to control. In consideration of comparable rates of FAO in hearts 24-36 h after sepsis induction and healthy hearts, this result appears conclusive. However, it is opposed by previously reported experiments using LPS injection instead. In a setup of neonatal sepsis, LPS were injected intraperitoneally to induce endotoxemia in suckling rats (Eaton et al. 2003, Fukumoto et al. 2002). CPT I activity was observed to be reduced two hours after injection in hearts from endotoxemic animals without affection of CPT II. Likewise, intraperitoneal injection of LPS in C57BL/6 mice resulted in a significant reduction of CPT I gene expression in the heart (Drosatos et al. 2013). Indeed, the down-regulation of CPT I was accompanied by significant impairment of cardiac function and additional reduction of FAO, indicating a different cardiac phenotype relative to our model. Further studies addressing CPT activities rather focused on hepatic CPT and reported varying results. In male Wistar rats, sepsis induced by CLP provoked an increase of CPT activity in liver (Yamamoto 1993). In contrast, another study observed decreased CPT activities and down-regulation of CPT gene expression in septic Sprague-Dawley rats after CLP (Barke et al. 1996). Therefore, CPT activity in context of sepsis remains controversial and appears to be dependent on the used model and species.

Although HCR hearts tended to oxidize more fatty acids than LCR hearts in this study, CPT I and II activity seemed not to be influenced by intrinsic exercise capacity. Increased CPT

activity could have in part explained the tendential rise in FAO seen in HCR. Previously, a 1.29-fold up-regulation of CPT I gene expression has been reported for cardiac tissue from HCR rats compared to LCR (Bye et al. 2008). Indeed, higher gene expression does not automatically result in increases in enzymatic activity due to action of a variety of regulatory factors. FAO is not exclusively governed by CPT activity but is controlled by a complex network of regulators. The indifferent CPT activities measured in this study imply the involvement of further mechanisms in the control of FAO in HCR and LCR hearts.

7 Conclusion

In the current study, the influence of sepsis on cardiac substrate metabolism and function in dependence of intrinsic exercise capacity was investigated for the first time. Induction of sepsis did not lead to disturbances of basal cardiac metabolism or mechanical dysfunction in our animal model. Insulin sensitivity of septic and post-septic hearts appeared preserved. Genetic predisposition for intrinsic exercise capacity did not affect substrate preference or cardiac performance, neither in acute sepsis nor in sepsis-survivors.

Therefore, the detrimental outcome of sepsis cannot be attributed to perturbances of cardiac substrate metabolism or function. The advantage in survival 24 h after sepsis induction previously seen in animals with high intrinsic exercise capacity did not correlate with metabolic or functional alterations in the heart; thus, the reasons responsible for this advantage remain elusive.

8 References

- Agwunobi AO, Reid C, Maycock P, Little RA, Carlson GL. 2000. Insulin resistance and substrate utilization in human endotoxemia. *J Clin Endocrinol Metab*, 85 (10):3770-3778.
- Akki A, Smith K, Seymour AM. 2008. Compensated cardiac hypertrophy is characterised by a decline in palmitate oxidation. *Mol Cell Biochem*, 311 (1-2):215-224.
- Allard MF, Schonekess BO, Henning SL, English DR, Lopaschuk GD. 1994. Contribution of oxidative metabolism and glycolysis to ATP production in hypertrophied hearts. *Am J Physiol*, 267 (2 Pt 2):H742-750.
- Barke RA, Birklid S, Chapin RB, Roy S, Brady PS, Brady LJ. 1996. The effect of surgical treatment following peritoneal sepsis on hepatic gene expression. *J Surg Res*, 60 (1):101-106.
- Beesley SJ, Weber G, Sarge T, Nikravan S, Grissom CK, Lanspa MJ, Shahul S, Brown SM. 2018. Septic Cardiomyopathy. *Crit Care Med*, 46 (4):625-634.
- Bertrand L, Horman S, Beauloye C, Vanoverschelde JL. 2008. Insulin signalling in the heart. *Cardiovasc Res*, 79 (2):238-248.
- Bieber LL, Abraham T, Helmrath T. 1972. A rapid spectrophotometric assay for carnitine palmitoyltransferase. *Anal Biochem*, 50 (2):509-518.
- Bierbrauer J, Weber-Carstens S. 2011. [Insulin resistance and protein catabolism in critically ill patients]. *Anesthesiol Intensivmed Notfallmed Schmerzther*, 46 (4):268-274; quiz 275.
- Bikman BT, Woodlief TL, Noland RC, Britton SL, Koch LG, Lust RM, Dohm GL, Cortright RN. 2009. High-fat diet induces Ikkbeta and reduces insulin sensitivity in rats with low running capacity. *Int J Sports Med*, 30 (9):631-635.
- Boudina S, Sena S, Theobald H, Sheng X, Wright JJ, Hu XX, Aziz S, Johnson JI, Bugger H, Zaha VG, Abel ED. 2007. Mitochondrial energetics in the heart in obesity-related diabetes: direct evidence for increased uncoupled respiration and activation of uncoupling proteins. *Diabetes*, 56 (10):2457-2466.
- Bradford MM. 1976. A rapid and sensitive method for the quantitation of microgram quantities of protein utilizing the principle of protein-dye binding. *Anal Biochem*, 72:248-254.

- Burniston JG, Kenyani J, Wastling JM, Burant CF, Qi NR, Koch LG, Britton SL. 2011. Proteomic analysis reveals perturbed energy metabolism and elevated oxidative stress in hearts of rats with inborn low aerobic capacity. *Proteomics*, 11 (16):3369-3379.
- Bye A, Langaas M, Hoydal MA, Kemi OJ, Heinrich G, Koch LG, Britton SL, Najjar SM, Ellingsen O, Wisloff U. 2008. Aerobic capacity-dependent differences in cardiac gene expression. *Physiol Genomics*, 33 (1):100-109.
- Chambrier C, Laville M, Rhzioual Berrada K, Odeon M, Bouletreau P, Beylot M. 2000. Insulin sensitivity of glucose and fat metabolism in severe sepsis. *Clin Sci (Lond)*, 99 (4):321-328.
- Chung HY, Kollmey AS, Schrepper A, Kohl M, Blass MF, Stehr SN, Lupp A, Graler MH, Claus RA. 2017. Adjustment of Dysregulated Ceramide Metabolism in a Murine Model of Sepsis-Induced Cardiac Dysfunction. *Int J Mol Sci*, 18 (4).
- Doenst T, Nguyen TD, Abel ED. 2013. Cardiac metabolism in heart failure: implications beyond ATP production. *Circ Res*, 113 (6):709-724.
- Doenst T, Han Q, Goodwin GW, Guthrie PH, Taegtmeyer H. 1998. Insulin does not change the intracellular distribution of hexokinase in rat heart. *Am J Physiol*, 275 (4 Pt 1):E558-567.
- Doenst T, Richwine RT, Bray MS, Goodwin GW, Frazier OH, Taegtmeyer H. 1999. Insulin improves functional and metabolic recovery of reperfused working rat heart. *Ann Thorac Surg*, 67 (6):1682-1688.
- Doenst T, Pytel G, Schrepper A, Amorim P, Farber G, Shingu Y, Mohr FW, Schwarzer M. 2010. Decreased rates of substrate oxidation ex vivo predict the onset of heart failure and contractile dysfunction in rats with pressure overload. *Cardiovasc Res*, 86 (3):461-470.
- Drosatos K, Drosatos-Tampakaki Z, Khan R, Homma S, Schulze PC, Zannis VI, Goldberg IJ. 2011. Inhibition of c-Jun-N-terminal kinase increases cardiac peroxisome proliferator-activated receptor alpha expression and fatty acid oxidation and prevents lipopolysaccharide-induced heart dysfunction. *J Biol Chem*, 286 (42):36331-36339.
- Drosatos K, Khan RS, Trent CM, Jiang H, Son NH, Blaner WS, Homma S, Schulze PC, Goldberg IJ. 2013. Peroxisome proliferator-activated receptor-gamma activation prevents sepsis-related cardiac dysfunction and mortality in mice. *Circ Heart Fail*, 6 (3):550-562.
- Dyson A, Rudiger A, Singer M. 2011. Temporal changes in tissue cardiorespiratory function during faecal peritonitis. *Intensive Care Med*, 37 (7):1192-1200.
- Eaton S, Fukumoto K, Stefanutti G, Spitz L, Zammit VA, Pierro A. 2003. Myocardial carnitine palmitoyltransferase I as a target for oxidative modification in inflammation and sepsis. *Biochem Soc Trans*, 31 (Pt 6):1133-1136.

- Fink MP. 2014. Animal models of sepsis. *Virulence*, 5 (1):143-153.
- Fleischmann C, Thomas-Rueddel DO, Hartmann M, Hartog CS, Welte T, Heublein S, Dennler U, Reinhart K. 2016. Hospital Incidence and Mortality Rates of Sepsis. *Dtsch Arztebl Int*, 113 (10):159-166.
- Fukumoto K, Pierro A, Spitz L, Eaton S. 2002. Differential effects of neonatal endotoxemia on heart and kidney carnitine palmitoyl transferase I. *J Pediatr Surg*, 37 (5):723-726.
- Geisser ME, Wang W, Smuck M, Koch LG, Britton SL, Lydic R. 2008. Nociception before and after exercise in rats bred for high and low aerobic capacity. *Neurosci Lett*, 443 (1):37-40.
- Gonnert FA, Recknagel P, Seidel M, Jbeily N, Dahlke K, Bockmeyer CL, Winning J, Losche W, Claus RA, Bauer M. 2011. Characteristics of clinical sepsis reflected in a reliable and reproducible rodent sepsis model. *J Surg Res*, 170 (1):e123-134.
- Goodwin GW, Ahmad F, Doenst T, Taegtmeier H. 1998. Energy provision from glycogen, glucose, and fatty acids on adrenergic stimulation of isolated working rat hearts. *Am J Physiol*, 274 (4 Pt 2):H1239-1247.
- Hall MJ, Williams SN, DeFrances CJ, Golosinskiy A. 2011. Inpatient care for septicemia or sepsis: a challenge for patients and hospitals. *NCHS Data Brief*, (62):1-8.
- Hinkle PC. 2005. P/O ratios of mitochondrial oxidative phosphorylation. *Biochim Biophys Acta*, 1706 (1-2):1-11.
- Hotamisligil GS, Peraldi P, Budavari A, Ellis R, White MF, Spiegelman BM. 1996. IRS-1-mediated inhibition of insulin receptor tyrosine kinase activity in TNF- α - and obesity-induced insulin resistance. *Science*, 271 (5249):665-668.
- Iliadis F, Kadoglou N, Didangelos T. 2011. Insulin and the heart. *Diabetes Res Clin Pract*, 93 Suppl 1:S86-91.
- Illuri VD, Layden BT, Aleppo G. 2016. Extreme Insulin Resistance in Critically Ill Patient With Sepsis. *Clin Diabetes*, 34 (3):158-160.
- Karwi QG, Uddin GM, Ho KL, Lopaschuk GD. 2018. Loss of Metabolic Flexibility in the Failing Heart. *Front Cardiovasc Med*, 5:68.
- Khadour FH, Panas D, Ferdinandy P, Schulze C, Csont T, Lalu MM, Wildhirt SM, Schulz R. 2002. Enhanced NO and superoxide generation in dysfunctional hearts from endotoxemic rats. *Am J Physiol Heart Circ Physiol*, 283 (3):H1108-1115.
- Koch LG, Britton SL. 2001. Artificial selection for intrinsic aerobic endurance running capacity in rats. *Physiol Genomics*, 5 (1):45-52.

- Koch LG, Meredith TA, Fraker TD, Metting PJ, Britton SL. 1998. Heritability of treadmill running endurance in rats. *Am J Physiol*, 275 (5 Pt 2):R1455-1460.
- Koch LG, Kemi OJ, Qi N, Leng SX, Bijma P, Gilligan LJ, Wilkinson JE, Wisloff H, Hoydal MA, Rolim N, Abadir PM, van Grevenhof EM, Smith GL, Burant CF, Ellingsen O, Britton SL, Wisloff U. 2011. Intrinsic aerobic capacity sets a divide for aging and longevity. *Circ Res*, 109 (10):1162-1172.
- Kumar A, Thota V, Dee L, Olson J, Uretz E, Parrillo JE. 1996. Tumor necrosis factor alpha and interleukin 1beta are responsible for in vitro myocardial cell depression induced by human septic shock serum. *J Exp Med*, 183 (3):949-958.
- Marik PE, Raghavan M. 2004. Stress-hyperglycemia, insulin and immunomodulation in sepsis. *Intensive Care Med*, 30 (5):748-756.
- McCowen KC, Ling PR, Ciccarone A, Mao Y, Chow JC, Bistrian BR, Smith RJ. 2001. Sustained endotoxemia leads to marked down-regulation of early steps in the insulin-signaling cascade. *Crit Care Med*, 29 (4):839-846.
- McDonough KH, Henry JJ, Lang CH, Spitzer JJ. 1986. Substrate utilization and high energy phosphate levels of hearts from hyperdynamic septic rats. *Circ Shock*, 18 (3):161-170.
- Mori J, Basu R, McLean BA, Das SK, Zhang L, Patel VB, Wagg CS, Kassiri Z, Lopaschuk GD, Oudit GY. 2012. Agonist-induced hypertrophy and diastolic dysfunction are associated with selective reduction in glucose oxidation: a metabolic contribution to heart failure with normal ejection fraction. *Circ Heart Fail*, 5 (4):493-503.
- Morris EM, Whaley-Connell AT, Thyfault JP, Britton SL, Koch LG, Wei Y, Ibdah JA, Sowers JR. 2009. Low aerobic capacity and high-fat diet contribute to oxidative stress and IRS-1 degradation in the kidney. *Am J Nephrol*, 30 (2):112-119.
- Neely JR, Morgan HE. 1974. Relationship between carbohydrate and lipid metabolism and the energy balance of heart muscle. *Annu Rev Physiol*, 36:413-459.
- Neubauer S. 2007. The failing heart--an engine out of fuel. *N Engl J Med*, 356 (11):1140-1151.
- Nguyen TD, Shingu Y, Amorim PA, Schwarzer M, Doenst T. 2015. Triheptanoin Alleviates Ventricular Hypertrophy and Improves Myocardial Glucose Oxidation in Rats With Pressure Overload. *J Card Fail*, 21 (11):906-915.
- Noland RC, Thyfault JP, Henes ST, Whitfield BR, Woodlief TL, Evans JR, Lust JA, Britton SL, Koch LG, Dudek RW, Dohm GL, Cortright RN, Lust RM. 2007. Artificial selection for high-capacity endurance running is protective against high-fat diet-induced insulin resistance. *Am J Physiol Endocrinol Metab*, 293 (1):E31-41.

- Palmieri V, Innocenti F, Guzzo A, Guerrini E, Vignaroli D, Pini R. 2015. Left Ventricular Systolic Longitudinal Function as Predictor of Outcome in Patients With Sepsis. *Circ Cardiovasc Imaging*, 8 (11):e003865; discussion e003865.
- Park EA, Cook GA. 1998. Differential regulation in the heart of mitochondrial carnitine palmitoyltransferase-I muscle and liver isoforms. *Mol Cell Biochem*, 180 (1-2):27-32.
- Parker MM, Shelhamer JH, Bacharach SL, Green MV, Natanson C, Frederick TM, Damske BA, Parrillo JE. 1984. Profound but reversible myocardial depression in patients with septic shock. *Ann Intern Med*, 100 (4):483-490.
- Paulson DJ, Ward KM, Shug AL. 1984. Malonyl CoA inhibition of carnitine palmitoyltransferase in rat heart mitochondria. *FEBS Lett*, 176 (2):381-384.
- Preiser JC, Zhang H, Vray B, Hrabak A, Vincent JL. 2001. Time course of inducible nitric oxide synthase activity following endotoxin administration in dogs. *Nitric Oxide*, 5 (2):208-211.
- Raymond RM, McLane MP, Law WR, King NF, Leutz DW. 1988. Myocardial insulin resistance during acute endotoxin shock in dogs. *Diabetes*, 37 (12):1684-1688.
- Recknagel P, Gonnert FA, Halilbasic E, Gajda M, Jbeily N, Lupp A, Rubio I, Claus RA, Kortgen A, Trauner M, Singer M, Bauer M. 2013. Mechanisms and functional consequences of liver failure substantially differ between endotoxaemia and faecal peritonitis in rats. *Liver Int*, 33 (2):283-293.
- Riehle C, Wende AR, Zaha VG, Pires KM, Wayment B, Olsen C, Bugger H, Buchanan J, Wang X, Moreira AB, Doenst T, Medina-Gomez G, Litwin SE, Lelliott CJ, Vidal-Puig A, Abel ED. 2011. PGC-1beta deficiency accelerates the transition to heart failure in pressure overload hypertrophy. *Circ Res*, 109 (7):783-793.
- Rittirsch D, Hoesel LM, Ward PA. 2007. The disconnect between animal models of sepsis and human sepsis. *J Leukoc Biol*, 81 (1):137-143.
- Rudiger A, Dyson A, Felsmann K, Carre JE, Taylor V, Hughes S, Clatworthy I, Protti A, Pellerin D, Lemm J, Claus RA, Bauer M, Singer M. 2013. Early functional and transcriptomic changes in the myocardium predict outcome in a long-term rat model of sepsis. *Clin Sci (Lond)*, 124 (6):391-401.
- Saddik M, Lopaschuk GD. 1991. Myocardial triglyceride turnover and contribution to energy substrate utilization in isolated working rat hearts. *J Biol Chem*, 266 (13):8162-8170.
- Schottmüller H. 1914. Wesen und Behandlung der Sepsis. *Inn Med*, 31:257-280.
- Schwarzer M, Britton SL, Koch LG, Wisloff U, Doenst T. 2010. Low intrinsic aerobic exercise capacity and systemic insulin resistance are not associated with changes in myocardial substrate oxidation or insulin sensitivity. *Basic Res Cardiol*, 105 (3):357-364.

- Sevilla Berrios RA, O'Horo JC, Velagapudi V, Pulido JN. 2014. Correlation of left ventricular systolic dysfunction determined by low ejection fraction and 30-day mortality in patients with severe sepsis and septic shock: a systematic review and meta-analysis. *J Crit Care*, 29 (4):495-499.
- Singer M, Deutschman CS, Seymour CW, Shankar-Hari M, Annane D, Bauer M, Bellomo R, Bernard GR, Chiche JD, Coopersmith CM, Hotchkiss RS, Levy MM, Marshall JC, Martin GS, Opal SM, Rubenfeld GD, van der Poll T, Vincent JL, Angus DC. 2016. The Third International Consensus Definitions for Sepsis and Septic Shock (Sepsis-3). *JAMA*, 315 (8):801-810.
- Soraya H, Masoud WG, Gandhi M, Garjani A, Clanachan AS. 2016. Myocardial mechanical dysfunction following endotoxemia: role of changes in energy substrate metabolism. *Basic Res Cardiol*, 111 (2):24.
- Standage SW, Bennion BG, Knowles TO, Ledee DR, Portman MA, McGuire JK, Liles WC, Olson AK. 2017. PPARalpha augments heart function and cardiac fatty acid oxidation in early experimental polymicrobial sepsis. *Am J Physiol Heart Circ Physiol*, 312 (2):H239-H249.
- Stanton T, Leano R, Marwick TH. 2009. Prediction of all-cause mortality from global longitudinal speckle strain: comparison with ejection fraction and wall motion scoring. *Circ Cardiovasc Imaging*, 2 (5):356-364.
- Taegtmeyer H, Lubrano G. 2014. Rethinking cardiac metabolism: metabolic cycles to refuel and rebuild the failing heart. *F1000Prime Rep*, 6:90.
- Taegtmeyer H, Young ME, Lopaschuk GD, Abel ED, Brunengraber H, Darley-Usmar V, Des Rosiers C, Gerszten R, Glatz JF, Griffin JL, Gropler RJ, Holzhuetter HG, Kizer JR, Lewandowski ED, Malloy CR, Neubauer S, Peterson LR, Portman MA, Recchia FA, Van Eyk JE, Wang TJ, American Heart Association Council on Basic Cardiovascular S. 2016. Assessing Cardiac Metabolism: A Scientific Statement From the American Heart Association. *Circ Res*, 118 (10):1659-1701.
- Tessier JP, Thurner B, Jungling E, Luckhoff A, Fischer Y. 2003. Impairment of glucose metabolism in hearts from rats treated with endotoxin. *Cardiovasc Res*, 60 (1):119-130.
- Tsolaki V, Makris D, Mantzaris K, Zakynthinos E. 2017. Sepsis-Induced Cardiomyopathy: Oxidative Implications in the Initiation and Resolution of the Damage. *Oxid Med Cell Longev*, 2017:7393525.
- Umbarawan Y, Syamsunarno M, Obinata H, Yamaguchi A, Sunaga H, Matsui H, Hishiki T, Matsuura T, Koitabashi N, Obokata M, Hanaoka H, Haque A, Kunitomo F, Tsushima Y, Suematsu M, Kurabayashi M, Iso T. 2017. Robust suppression of cardiac energy catabolism with marked accumulation of energy substrates during lipopolysaccharide-induced cardiac dysfunction in mice. *Metabolism*, 77:47-57.

- Unuma K, Aki T, Nagano S, Watanabe R, Uemura K. 2018. The down-regulation of cardiac contractile proteins underlies myocardial depression during sepsis and is mitigated by carbon monoxide. *Biochem Biophys Res Commun*, 495 (2):1668-1674.
- Watts JA, Kline JA, Thornton LR, Grattan RM, Brar SS. 2004. Metabolic dysfunction and depletion of mitochondria in hearts of septic rats. *J Mol Cell Cardiol*, 36 (1):141-150.
- Wisloff U, Najjar SM, Ellingsen O, Haram PM, Swoap S, Al-Share Q, Fernstrom M, Rezaei K, Lee SJ, Koch LG, Britton SL. 2005. Cardiovascular risk factors emerge after artificial selection for low aerobic capacity. *Science*, 307 (5708):418-420.
- Yamamoto T. 1993. Rat liver peroxisomal and mitochondrial fatty acid oxidation in sepsis. *Surg Today*, 23 (2):137-143.
- Yang N, Shi XL, Zhang BL, Rong J, Zhang TN, Xu W, Liu CF. 2018. The Trend of beta3-Adrenergic Receptor in the Development of Septic Myocardial Depression: A Lipopolysaccharide-Induced Rat Septic Shock Model. *Cardiology*, 139 (4):234-244.
- Zhabyeyev P, Gandhi M, Mori J, Basu R, Kassiri Z, Clanachan A, Lopaschuk GD, Oudit GY. 2013. Pressure-overload-induced heart failure induces a selective reduction in glucose oxidation at physiological afterload. *Cardiovasc Res*, 97 (4):676-685.

9 Appendix

9.1 List of figures

Figure 1: Exercise performance assessed in HCR and LCR rats after 22 generations of divergent selection.	13
Figure 2: Influence of intrinsic exercise capacity on sepsis survival.....	14
Figure 3: Carnitine palmitoyltransferase system.....	17
Figure 4: Biochemistry of the radioactive tracers [U- ¹⁴ C]-glucose and [9,10- ³ H]-oleate	19
Figure 5: Experimental setup of the isolated working rat heart	27
Figure 6: Perfusion protocol.....	29
Figure 7: Morphological parameters	34
Figure 8: Cardiac power of HCR and LCR hearts over time	35
Figure 9: Cardiac performance assessed during isolated working heart perfusions	36
Figure 10: Baseline cardiac glucose oxidation	37
Figure 11: Cardiac glucose oxidation after administration of insulin.....	38
Figure 12: Baseline cardiac fatty acid oxidation.....	39
Figure 13: Cardiac fatty acid oxidation after administration of insulin	40
Figure 14: Ratio of glucose oxidation to fatty acid oxidation.....	41
Figure 15: Cardiac efficiency expressed as ratio of ATP production to cardiac power.....	42
Figure 16: Cardiac CPT I and II activities.....	43

9.2 Ehrenwörtliche Erklärung

Hiermit erkläre ich, dass mir die Promotionsordnung der Medizinischen Fakultät der Friedrich-Schiller-Universität bekannt ist,

ich die Dissertation selbst angefertigt habe und alle von mir benutzten Hilfsmittel, persönlichen Mitteilungen und Quellen in meiner Arbeit angegeben sind,

mich folgende Personen bei der Auswahl und Auswertung des Materials sowie bei der Herstellung des Manuskripts unterstützt haben: Prof. Dr. Torsten Doerst, Dr. Michael Schwarzer,

die Hilfe eines Promotionsberaters nicht in Anspruch genommen wurde und dass Dritte weder unmittelbar noch mittelbar geldwerte Leistungen von mir für Arbeiten erhalten haben, die im Zusammenhang mit dem Inhalt der vorgelegten Dissertation stehen,

dass ich die Dissertation noch nicht als Prüfungsarbeit für eine staatliche oder andere wissenschaftliche Prüfung eingereicht habe und

dass ich die gleiche, eine in wesentlichen Teilen ähnliche oder eine andere Abhandlung nicht bei einer anderen Hochschule als Dissertation eingereicht habe.

Ort, Datum

Unterschrift des Verfassers

9.3 Acknowledgement

Die folgenden Zeilen sind all Jenen gewidmet, die die Entwicklung dieser Arbeit couragiert begleitet und maßgeblich zu deren erfolgreichen Fertigstellung beigetragen haben.

Zunächst möchte ich Herrn Prof. Torsten Doerst meinen herzlichsten Dank für die Bereitstellung des Promotionsthemas und die Integration in seine Arbeitsgruppe aussprechen. Er hat meine Begeisterung für die grundlagenwissenschaftliche Erforschung des Herzstoffwechsels früh mit seiner Leidenschaft geweckt und unterstützte alle meine Vorhaben stets mit bemerkenswertem Engagement.

Besonderer Dank gilt Herrn Dr. Michael Schwarzer für die wissenschaftliche Begleitung der experimentellen Arbeiten und die Revision des Manuskriptes. Seine ständige Bereitschaft, aufkommende Fragen und Probleme kritisch zu diskutieren und zuweilen Denkanstöße zu geben, war von essentieller Bedeutung für die Entstehung dieser Dissertationsschrift.

Weiterhin danke ich allen Laborkollegen, insbesondere Herrn Dr. Tien Dung Nguyen, Frau Dr. Andrea Schrepper, Frau Dr. Christina Schenkl und Frau Estelle Heyne, für ihre tatkräftige Hilfe im Laboralltag und ihre geduldige Einweisung in die Methodik.

Schließlich möchte ich meinen Eltern, Großeltern, meinem Bruder, meiner Freundin und allen Verwandten und Freunden herzlichst für ihre hingebungsvolle und ungebremschte Unterstützung danken, die sie mir nicht nur während der Arbeit an dieser Dissertation, sondern auch im gesamten Studium haben zu Teil werden lassen.